



**João Frederico Lourenço dos Santos Barata
Morgado**

Licenciado em Bioquímica

**Preparation of biopolymer-drug
formulations for cancer drug delivery**

Dissertação para obtenção do Grau de Mestre em
Bioquímica

Orientador: Doutora Maria Filomena Andrade de Freitas
Investigadora sénior, FCT-UNL

Co-orientador: Maria Alexandra Núncio de Carvalho
Ramos Fernandes, Professora Doutora, FCT/UNL

Júri:

Presidente: Prof. Doutor Pedro António de Brito Tavares
Arguente: Prof. Doutor Vítor Manuel Delgado Alves
Vogal: Prof. Doutora Maria Filomena Andrade de Freitas



FACULDADE DE
CIÊNCIAS E TECNOLOGIA
UNIVERSIDADE NOVA DE LISBOA

Setembro de 2018



**João Frederico Lourenço dos Santos Barata
Morgado**

Licenciado em Bioquímica

**Preparation of biopolymer-drug
formulations for cancer drug delivery**

Dissertação para obtenção do Grau de Mestre em
Bioquímica

Orientador: Doutora Maria Filomena Andrade de Freitas
Investigadora sénior, FCT-UNL

Co-orientador: Maria Alexandra Nuncio de Carvalho
Ramos Fernandes, Professora Doutora, FCT/UNL

Júri:

Presidente: Prof. Doutor Pedro António de Brito Tavares
Arguente: Prof. Doutor Vítor Manuel Delgado Alves
Vogal: Prof. Doutora Maria Filomena Andrade de Freitas



FACULDADE DE
CIÊNCIAS E TECNOLOGIA
UNIVERSIDADE NOVA DE LISBOA

Setembro de 2018

Copyright

“Preparation of biopolymer-drug formulations for cancer drug delivery”

Copyright © João Frederico Lourenço dos Santos Barata Morgado, Faculdade de Ciências e Tecnologia, Universidade Nova de Lisboa

A Faculdade de Ciências e Tecnologia e a Universidade Nova de Lisboa têm o direito, perpétuo e sem limites geográficos, de arquivar e publicar esta dissertação através de exemplares impressos reproduzidos em papel ou de forma digital, ou por qualquer outro meio conhecido ou que venha a ser inventado, e de a divulgar através de repositórios científicos e de admitir a sua cópia e distribuição com objetivos educacionais ou de investigação, não comerciais, desde que seja dado crédito ao autor e editor.

Acknowledgements

First of all, I would like to thank my thesis advisor, Dr. Filomena Freitas, for all the knowledge and know-how shared over the course of this thesis, for all the patience and availability demonstrated to me, for always cheering me up whenever things didn't work out, and for always promptly devising new ways to keep this thesis moving forward towards proper completion, despite all the bad results obtained.

I would also like to thank my thesis co-advisor, Dr. Alexandra Fernandes, for always pushing me to think on my own rather than depending solely on my advisors, which made me grow as a person and a scientist, for the patience to always answer to my questions whenever I couldn't get there alone, no matter how dull they were, and for all the new ideas devised when confronted with my bad results, which kept me moving forward.

To both my advisors, thank you very much.

A special thanks goes to Dr. Pedro Viana Batista, for helping me think outside the box and showing me that a bad result is just a matter of perspective.

I would like to leave a thank you to all the people in the two research groups I have been a part of during this year, BioEng and Human Genetics and Cancer Therapeutics, especially to João Pereira, Diana Araújo, Sílvia Baptista, Inês Farinha, Patrícia Reis, Patrícia Freitas, Cristiana Torres (of the BioEng group), Catarina Roma-Rodrigues, Luis Raposo, Andreia Carvalho and Catarina Brás (of the Human Genetics and Cancer Therapeutics) for integrating me in their respective groups, for all the brainstorming, discussions and advices given, as well as for the support provided to me in completing this thesis.

A thank you to my fellow master students in both research groups, Joana Almeida (Human Genetics and Cancer Therapeutics group), Bruno Guerreiro, Patrícia Serrano and Ana Teresa (BioEng) for all the companionship shown to me over this year.

A word of appreciation also to Ana Teresa, Mariana Matos and Liane Meneses for supplying me with the mixed cultures biomass for PHAs extraction, as well as some already extracted polymer.

To my family, which has supported me all my life, inciting me to pursue my dreams, a very heartfelt thank you. For all their invaluable support over my academic course, both during and before college, and for always being there for me, thank you.

Finally, to my girlfriend, Magda Ferreira, for all her love and support, for all the hours spent hearing me rambling and thinking out loud, for all the ideas and brainstorms, for all the nights spent awake on my expense, for all the troubles she went through, for helping me in every way she could, thank you very much.

Abstract

Mannans are highly water-soluble mannose heteropolymers produced by a number of organisms, including yeasts. Polyhydroxyalkanoates (PHAs) are aliphatic polyesters produced by numerous bacteria as a carbon and energy source, with interesting thermal and mechanical properties.

The main objective of this thesis was to prepare different polymeric structures base on mannans and PHAs for use in the pharmaceutical and biomedical areas. Mannans were produced by *Komagataella pastoris* using glycerol as carbon source, extracted with a heat-alkali treatment and purified using dialysis. PHAs were produced by mixed cultures using fermented fruit pulp waste, extracted using chloroform or hypochlorite and purified in ethanol.

A successful deproteinization and an unsuccessful phosphorylation procedure was performed in mannans. The results show a decrease in protein content of 69.49 ± 0.44 % and a decrease in phosphate content of 60.45 ± 1.23 %, respectively.

Mannans were tested in normal fibroblasts, HCT116 and A2780 cell lines for their cytotoxicity, by MTS assay, and no cytotoxicity was discovered. They were then used to prepare gel structures, and gelled using di- and tri-valent cations of iron and copper at low temperature (4 °C) and alkaline pH. Gel particles were obtained in the above conditions and tested for their stability in water. Particles made using tri-valent iron were found the most stable.

Mannans were also used to produce films. Films were obtained from i) mannans in water dried at 30 °C or freeze dried, ii) from the previously produced films (30 °C) and then coated with iron, at neutral pH or followed by immersion in an alkaline solution and, iii) from gel beads dried at 30 °C or freeze dried. Films were tested for cell adhesion *in vitro* using normal fibroblasts, but no positive results were found.

PHAs with different HV ratios were used to produce films, pure and blended with mannans, using chloroform as solvent by a solvent casting method. The produced films were tested for cell adhesion *in vitro*, using fibroblasts and MCF7-GFP. Pure PHA films were deemed good matrices for this application with cells adherent to their surface, whereas blend matrices failed in this regard. Some pure PHA matrices were then tested for their cytotoxicity using MCF7-GFP, and with the exception of co-polymer PHBHV with HV content of 18 % (extracted with hypochlorite), they were found to be non-cytotoxic, rendering them useful for biomedical applications such as wound dressing or drug delivery.

Keywords: Mannans; Polyhydroxyalkanoates; Mannans gel beads; Polymeric Films; Cytotoxicity assays; Cell adherence assays.

Resumo

Mananos são heteropolímeros de manose altamente solúveis em água produzidos por vários organismos, incluindo leveduras. Polihidroxialcanoatos (PHAs) são poliésteres alifáticos produzidos por diversas bactérias como fonte de carbono e energia, com interessantes propriedades térmicas e mecânicas.

O principal objetivo desta tese foi preparar diferentes estruturas poliméricas baseadas em mananos e PHAs para uso nas áreas farmacêutica e biomédica. Os mananos foram produzidos por *Komagataella pastoris* usando glicerol como fonte de carbono, extraídos com um tratamento térmico e alcalino, e purificados por diálise. Os PHA foram produzidos por culturas mistas utilizando resíduos de polpa de fruta fermentada, extraídos usando clorofórmio ou hipoclorito e purificados em etanol.

Foi realizada em mananos uma desproteínização com sucesso e um procedimento de fosforilação sem sucesso. Os resultados mostram uma diminuição no conteúdo em proteína de $69,49 \pm 0,44$ % e uma diminuição no conteúdo em fosfato de $60,45 \pm 1,23$ %, respectivamente.

Os mananos foram testados em fibroblastos normais e nas linhas celulares HCT116 e A2780 para avaliar a sua citotoxicidade, através de um ensaio MTS, e não foi descoberta nenhuma citotoxicidade. Estes foram então usados para preparar estruturas de gel, e gelificaram usando catiões di- e trivalentes de ferro e cobre a baixa temperatura (4 °C) e pH alcalino. As partículas de gel foram obtidas nas condições acima e testadas quanto à sua estabilidade em água. As partículas feitas com ferro trivalente foram consideradas as mais estáveis.

Este polímero foi ainda utilizado para produzir filmes. Os filmes foram obtidos de i) mananos em água, secos a 30 °C ou liofilizados, ii) filmes produzidos anteriormente (30 °C) e revestidos com ferro, a pH neutro ou seguidos de imersão em solução alcalina e, iii) esferas de gel secas a 30 °C ou liofilizadas. Estes filmes foram testados quanto à adesão celular *in vitro* utilizando fibroblastos normais, mas não foram encontrados resultados positivos.

Foram utilizados PHAs com diferentes rácios de HV para produzir filmes, puros e misturados com mananos, utilizando clorofórmio como solvente. Os filmes produzidos foram testados quanto à adesão celular *in vitro*, utilizando fibroblastos e MCF7-GFP. Os filmes de PHA puro foram considerados boas matrizes para esta aplicação, com células aderentes à sua superfície, enquanto que nas matrizes de mistura se verificou pouca adesão celular. Algumas matrizes de PHA puro foram então testadas quanto à sua citotoxicidade usando MCF7-GFP e, com exceção do co-polímero PHBHV com teor de HV de 18 % (extraído com hipoclorito), verificou-se não serem citotóxicas, tornando-se úteis para aplicações biomédicas tais como revestimento de feridas e libertação controlada de fármacos.

Palavras-chave: Mananos; Polihidroxialcanoatos; Partículas de gel de mananos; Filmes poliméricos; Ensaio de viabilidade celular; Ensaio de adesão celular.

Index

Acknowledgements.....	vii
Abstract.....	ix
Resumo.....	xi
Index	xiii
Index of figures	xv
Index of tables.....	xvii
List of abbreviations.....	xix
Chapter 1. Introduction	1
1.1. Natural Polymers	1
1.1.1. Polysaccharides.....	1
1.1.2. Yeast Polysaccharides	2
1.1.3. Mannans and Mannoproteins	2
1.1.4. Polyesters	4
1.1.5. Polyhydroxyalkanoates.....	4
1.2. Polysaccharide Gels	6
1.2.1. Gel Particles	6
1.3. Polymeric Films	7
1.4. Motivation	7
Chapter 2. Materials and Methods	9
2.1. Polysaccharide	9
2.1.1. Polysaccharide Production	9
2.1.1.1. Inoculum Preparation	9
2.1.1.2. Bioreactor Assay.....	9
2.1.1.3. Analytical Techniques.....	9
2.1.2. Polysaccharide Extraction and Purification	10
2.1.3. Polysaccharide Characterization	10
2.1.3.1. Monomeric Analysis	10
2.1.3.2. Protein Quantification	11
2.1.3.3. Moisture Content	11
2.1.3.4. Inorganic Content	11
2.1.3.5. Elemental Analysis	11
2.1.3.6. Phosphate Content.....	11
2.1.4. Polysaccharide Transformation	12
2.1.4.1. Deproteination	12
2.1.4.2. Phosphorylation	12
2.2. Polyester.....	12
2.2.1. Polyester Extraction and Purification.....	12
2.3. Biopolymer Matrices	13
2.3.1. Gelation Procedures.....	13

2.3.2. Film Formation Procedures	14
2.4. Cell Cultures	17
2.5. Cytotoxicity Assays.....	17
2.6. Cell Adherence Assays	18
Chapter 3. Results and Discussion	19
3.1. Polysaccharide Production	19
3.2. Polysaccharide Characterization	19
3.2.1. Monomeric Analysis	19
3.2.2. Protein Quantification	20
3.2.3. Moisture Content	20
3.2.4. Inorganic Content	20
3.2.5. Elemental Analysis	20
3.2.6. Phosphate Content.....	21
3.3. Polysaccharide Transformation	21
3.3.1. Deproteination	21
3.3.2. Phosphorylation	22
3.4. Polyester Extraction and Purification.....	22
3.5. Biopolymer Matrices	23
3.5.1. Gelation Procedures.....	23
3.5.2. Film Formation Procedures	27
3.5.2.1. Polysaccharide Films.....	27
3.5.2.2. Polyester Films	29
3.6. Cytotoxicity Assays.....	32
3.7. Cell Adherence Assays	34
3.7.1. Polysaccharide Films.....	34
3.7.2. Polyester Films	36
Chapter 4. Conclusions and Future Work	47
Chapter 5. Bibliography	49

Index of figures

Figure 1.1. Simplified scheme for the formation of yeast cell wall components.....	3
Figure 1.2. Simplified PHA biosynthesis metabolic pathway.	5
Figure 2.1. Film formation procedures.	16
Figure 3.1. Cell Dry Weight over the course of the bioreactor assay.	19
Figure 3.2. Effect of pH and salt concentration on mannans gelation at 4 °C.	24
Figure 3.3. Beads resulting from different versions employed for structured gel particles formation. ..	25
Figure 3.4. Early stage mannans films obtained in teflon plates.	28
Figure 3.5. Plain mannans films obtained in petri dish and cell culture plate scale.	28
Figure 3.6. Methods for PHA/mannans films preparation.	30
Figure 3.7. Different polymeric ratios for film formation.	30
Figure 3.8. Some PHA films prepared for biological assays.	31
Figure 3.9. Mannans influence in cell viability.	32
Figure 3.10. Mannans influence in normal skin fibroblast cell viability (high concentrations).	33
Figure 3.11. Mannans films used in cell adherence assays.	35
Figure 3.12. Microscopic observation of MnOriFeNaOHHFilm after the cell adherence period (24 h). ..	36
Figure 3.13. Cell growth in 100PHB films.	38
Figure 3.14. Cell growth in 75PHB films.	38
Figure 3.15. Cell growth in 100PHBHV17 films.	39
Figure 3.16. Cell growth in 75PHBHV17 films.	39
Figure 3.17. Cell growth in 100PHBHV18 films.	40
Figure 3.18. Cell growth in 75PHBHV18 films.	40
Figure 3.19. Cell growth in 100PHBHV27 films.	41
Figure 3.20. Cell growth in 75PHBHV27 films.	41
Figure 3.21. Cell growth in 100PHBHV38 films.	42
Figure 3.22. Cell growth in 75PHBHV38 films.	42
Figure 3.23. Cell growth in 100PHBHV56 films.	43
Figure 3.24. Cell growth in 75PHBHV56 films.	43
Figure 3.25. Cell viability of adherent MCF7-GFP cells in different PHA films.	44

Index of tables

Table 3.1. Elemental analysis of mannans.....	20
Table 3.2. Phosphate and ammonia content of mannans.....	21
Table 3.3. Effect of pH and temperature on mannans solutions gelation.	23
Table 3.4. Effect of pH and salt presence on mannans gelation at 4 °C.....	23
Table 3.5. Effect of pH and salt concentration on mannans gelation at 4 °C.....	24
Table 3.6. Different versions employed for structured gel particles formation.	25
Table 3.7. Mannans films prepared for biological assays.	29

List of abbreviations

(M6P)-IGF I	Mannose 6-phosphate/insulin-like growth factor II receptor
3D-printing	Three-dimensional printing
A2780	Ovarian carcinoma cell line
ATCC®	American type culture collection
BC	Bacterial cellulose
<i>C. albicans</i>	<i>Candida albicans</i>
CAD	Computer-aided design
CDW	Cell dry weight
CGC	Chitin-glucan complexes
ChGC	Chitosan-glucan complexes
DMEM	Dulbecco's modified eagle medium
DMSO	Dimethyl sulfoxide
DO	Dissolved oxygen
DOX	Doxorubicin
dsDNA	Double-stranded deoxyribonucleic acid
EPS	Exopolysaccharide
FBS	Fetal bovine serum
GDP-Man	Guanosine diphosphate mannose
GFP	Green fluorescent protein
HB	3-hydroxybutyrate
HCT116	Colorectal carcinoma cell line
HPLC	High pressure liquid chromatography
HV	3-hydroxyvalerate
ICP-AES	Inductively coupled plasma atomic emission spectroscopy
<i>K. pastoris</i>	<i>Komagataella pastoris</i>
lcl-PHA	Long-chain length PHA
M6P	Mannose 6-phosphate
MCF7-GFP	Modified breast adenocarcinoma cell line
mcl-PHA	Medium-chain length PHA
MEM	Minimum essential media
MnOri	Original mannans
MnProt	Deproteinized mannans
	3-(4,5-Dimethylthiazol-2-yl)-5-(3-carboxymethoxyphenyl)-2-(4-sulfophenyl)-
MTS	2H-tetrazolium
MWCO	Molecular weight cut-off
n.a.	Not available/ not tested
OD	Optical density
P(3-HB-co-4-HB)	Poly(3-hydroxybutyrate-co-4-hydroxybutyrate)
P(3-HB-co-4-HB)-BC	Poly(3-hydroxybutyrate-co-4-hydroxybutyrate)-bacterial cellulose

<i>P. holstii</i>	<i>Pichia holstii</i>
PCL	Poly(ϵ -caprolactone)
PEG	Polyethylene glycol 4000
PET	Polyethylene terephthalate
PHA	Polyhydroxyalkanoate
PHB	Poly-3-hydroxybutyrate
PHB-BC	Poly-3-hydroxybutyrate-bacterial cellulose
PHBHV	Poly-3-hydroxybutyrate-3-hydroxyvalerate
PLA	Poly(lactic acid)
PMS	Phenazinemethosulfate
pO₂	Dissolved oxygen concentration
pp	Precipitate
RH	Relative humidity
RPMI	Roswell Park Memorial Institute medium
scl-PHA	Short-chain length PHA
SD	Standard deviation
TCA	Trichloroacetic acid
TFA	Trifluoroacetic acid
TGF-β1	Transforming growth factor beta 1
UV	Ultraviolet
UV-Vis	Ultraviolet-visible

Chapter 1. Introduction

1.1. Natural Polymers

Many polymers of both natural and synthetic origin have been proposed and used in a variety of applications, including biomedical applications [1]. Natural polymers present an array of interesting properties suitable for diverse applications, which investigators have tried to replicate in the course of producing synthetic polymers. The natural counterparts, however, have been refined for billions of years, and are therefore still ahead [2].

Natural polymers are called so regarding their biotic origin, commonly being produced in animals or plants, but also in microorganisms. In fact, the interest in microbial products has been, and still is, increasing [3].

Regarding these biopolymers, three different macrostructures arise, comprising polysaccharides, polyesters and proteins [1, 4]. While undoubtedly important, the latter category falls out of interest to the purpose of this thesis, and will therefore be disregarded.

1.1.1. Polysaccharides

Polysaccharides can either be homopolymers or heteropolymers, respective to their chemical composition. Homopolymers (homopolysaccharides) are constituted by a single repeating monomer, the most common example being glucose homopolysaccharides (such as cellulose) [5]. Heteropolymers (heteropolysaccharides) are constituted by multiple different monomers, in various proportions. Glucose, galactose or rhamnose are among the most common monomers, but other monomers are also often found, such as mannose, N-acetylglucosamine or non-carbohydrate substituents, such as phosphate or glycerate [5].

Many naturally occurring polysaccharides from various origins (plant, algae, crustacean, fungal and bacterial) have been extensively studied and are currently being used in commercial products in different areas (food, pharmaceutical, cosmetic industry, among others), replacing synthetic polymers, as these natural polymers are more biodegradable, biocompatible and non-toxic. Some examples include Arabic gum (plant), carrageenan (algae), cellulose (plant, microbial), xanthan gum or gellan gum (microbial) [6].

Some of these natural sources of polysaccharides (plants, algae and crustacean), however, present meaningful drawbacks in terms of production and polymer extraction, either caused by seasonal constraints (long-term, unreliable productions, both regarding quantity and quality) or expensive purification methods to remove toxic or allergenic natural components, which may otherwise render the polymers inadequate for human use. Microbial polysaccharide production, on the other hand, can be more easily controlled and manipulated. Modern bioengineering techniques can achieve reproducible and high yielding polymer productions, in faster growth and production periods, while

sometimes couple those advantages with the use of cheap carbon sources obtained from industrial wastes and by-products [7].

Moreover, biopolymers obtained from microbial sources may comprise a series of inherent mechanical properties (such as gelling capacity, emulsifier, thickener, pH and thermal stability or film forming capacity), as well as functional properties (immune response increase, antimicrobial activity, antimutagenic activity, antitumor activity, among others), and can even be modulated (for example, novel chemical groups or metal addition for specific properties) to achieve intensified or novel properties [3, 8–10].

1.1.2. Yeast Polysaccharides

Yeast polysaccharides have been studied over the last few years, and the many properties ascertained so far have led to their proposal for healthcare related purposes, namely in pharmaceutical and biomedical applications, despite their clinical use still not being widespread [3].

These polymers can be categorized in mainly three types of polymers: cell-wall polysaccharides, capsular and extracellular polysaccharides. Extracellular polysaccharides are synthesized inside the yeast cell, and then transported to the extracellular environment. They can remain free in the medium (EPS) to form an involving matrix to support and protect the culture, as well as provide a means to interact with a possible host, or remain attached to the fungi cell wall (capsular polysaccharides) to confer an extra layer of protection [3].

Cell-wall polysaccharides are almost ubiquitous among yeast, composed of an outer layer of mannans and mannoproteins and an inner layer of D-glucans, chitin and chitosan and their respective complexes with glucans, chitin-glucan complexes (CGC), and chitosan-glucan complexes (ChGC) [3]. The cell-wall polysaccharides have various purposes. The inner layer is mostly responsible for structural support of the yeast cell, accounting for its stability [11]. CGC connects to a network of different glucans, providing some flexibility to the cell wall, as well as functioning as structural elements connecting the rigid CGC shell to the outer mannans and mannoproteins layer [12].

1.1.3. Mannans and Mannoproteins

The outer layer of the yeast cell wall is composed of mannans and mannoproteins and is an amorphous matrix of mannose heteropolymers. In yeast cells, these polysaccharides and glycoproteins have many functions, such as controlling the cell wall permeability or interacting with the medium. In some pathogenic strains, such as *Candida albicans*, they are used by the yeast to adhere to surfaces [13].

Mannose backbone chains, which may also contain other sugars, such as glucose or galactose (called

glucomannans or galactomannans, respectively), are linked by α -1,3-, α -1,6-, β -1,3- and β -1,4-glycosidic links. Mannans backbones are often highly branched, presenting an even vaster array of sugar side chains and their substituents, such as glucose and galactose, but also fucose, xylose, mannose and glucuronic acids, as well as non-carbohydrate versions of the previous (such as phosphorylated versions), to name a few. Some yeast mannans have been reported to have mannose contents over 90 % [3].

Mannoproteins are glycoproteins constituted by a central protein linked to two side chains of heteropolymer mannan, a long chain (usually up to 100 monomers) which is highly branched, and a smaller chain with usually no more than 5 monomers, which are linked to the central protein through asparagine and threonine or serine residues, respectively. Mannans and mannoproteins are produced in the endoplasmic reticulum from a nucleotide diphosphate mannose, GDP-Man. Mannosyl residues are obtained from GDP-Man by mannosyltransferases, which are then linked together in a linear form and bound to the proteins. The glycoproteins are then conducted to the cell wall by proper vesicles [3]. A scheme comprising the formation of yeast cell wall components is presented on figure 1.1.

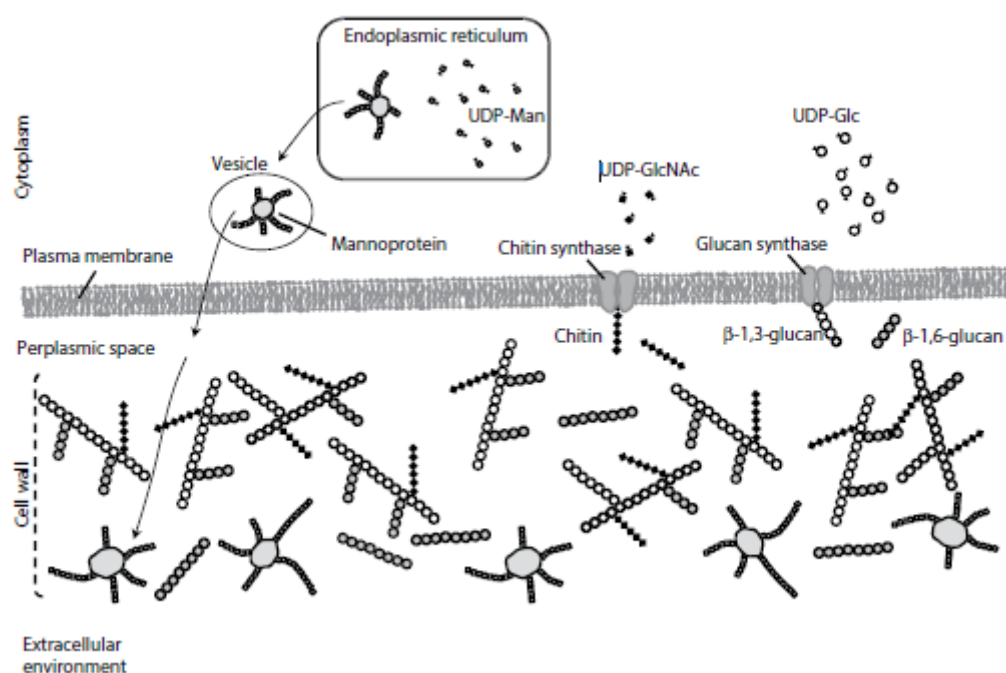


Figure 1.1. Simplified scheme for the formation of yeast cell wall components.
Adapted from Freitas et al. [3].

Many different kinds of mannans are naturally produced, with different biological activity properties, including immunomodulator, antimicrobial, antiviral, antioxidant or antimutagenic activity. Remarkably so, phosphomannans (mannans with a high presence of diester phosphate linked side chains) have been proved to possess antitumoral effect, especially when chemically modified to include other substituents such as sulphates [14, 15].

1.1.4. Polyesters

Polyesters are polymers whose repetitive units are bound together by ester linkages [16, 17]. They are usually obtained by esterification of dicarboxylic acids and dihydroxyl alcohols, and esterification can occur on either end of the molecules, allowing for vast polymeric chains to be produced [18]. Trihydroxyl alcohols and tricarboxylic acids can also be used, with esterification occurring in multiple sites, in which case the resulting polymer has a chance to contain crosslinks in its structure [18]. Polyesters can be divided into aliphatic and aromatic. Aromatic polyesters are polyesters which contain aromatic residues in their structure, whether part of the original monomers or co-polymerized with it [19]. These aromatic residues are responsible for the polymers lack of biodegradability, as most enzymes' active center cannot fit the cyclic carbon structure of the aromatic and therefore degrade the polymer [20]. The most notorious example of aromatic polyesters is polyethylene terephthalate (PET), commonly used in the food industry to produce plastic PET bottles [18].

Aliphatic polyesters are usually regarded as polymers with high biocompatibility and biodegradability/bioresorbability, and have therefore been proposed in numerous applications in the medical field, such as sutures, drug delivery vehicles, tissue engineering or implants [21, 22], as well as in food and agriculture fields as packaging materials. These polymers include polylactic acid (PLA) and poly(ϵ -caprolactone) (PCL) which are commercially available, but also other polymers with interesting properties such as polyhydroxyalkanoates (PHAs) [16].

1.1.5. Polyhydroxyalkanoates

Polyhydroxyalkanoates (PHAs) are naturally occurring aliphatic polyesters produced by some organisms, including bacteria, as a carbon and energy source. PHAs are synthesized intracellularly by a cascade of enzymatic reactions (figure 1.1). Upon production, PHAs are accumulated in the form of granules in the cytoplasm, surrounded by a monolayer of phospholipids and associated proteins [17, 23]. PHAs can be composed of numerous monomers, which lends co-polymers of these monomers a wide range of physical and thermal properties, including ones that resemble petrochemical-derived polymers currently used in the industry, such as polypropylene or polyethylene [23, 24]. Regarding monomer size, PHAs can be divided in three categories: short-chain length PHA (scl-PHA), with monomers composed of 5 or less carbon units, medium-chain length PHA (mcl-PHA), with monomers ranging from 6 to 14 carbon atoms, and long-chain length PHA, with monomers composed of over 14 carbon atoms. The most common PHAs currently studied are scl-PHA, in which 3-hydroxybutyrate (HB) and 3-hydroxyvalerate (HV) monomers are included [23]. Poly(3-hydroxybutyrate) (PHB) is a scl-PHA homopolymer composed only of HB monomers and is produced by, among others, *Cupriavidus necator* (formerly *Ralstonia eutropha* H16) [24, 25]. This bacterium has also been described to incorporate HV in this polymer, producing a co-polymer poly(3-hydroxybutyrate-co-3-hydroxyvalerate) (PHBHV). This co-polymer has increased mechanical properties when compared to PHB (such as improved ductility), similar to those of PLA, and is now commercially available [26].

Mixed cultures have also been used to produce PHAs. Advantages of this PHA production method include less control steps required for its production, such as sterilization or pH control, and an efficient valorization of wastes, which in turn may lower the overall production costs. Other steps may be necessary, however, such as transformation of the carbon source, as typical carbohydrate substrates may be converted in different products. In such cases, a simple fermentation of the carbon source could be used, yielding fatty acids which are preferential for PHA production [27]. Organisms that accumulate PHA as a carbon and energy stock are naturally selected from the mixed cultures due to their higher adaptability to nutrient variations, and the culture is constantly adapting to the changes in the medium. This is especially useful since mixed cultures PHA production was initially thought for waste water treatment systems, in which medium variability plays an important role in bacterial survival, and accumulated PHA is also a metabolic intermediate to the waste water treatment process by these bacteria [28]. PHAs produced by mixed cultures vary according to the feedstock supplied and may be homopolymers such as pure PHB, or co-polymers such as P(3-HB-co-3-HV) with reported HV contents as high as 82 % [28].

The incorporation of PHAs in the industry, however desirable their properties are, is still going at a slow pace due to their production costs, most notably the recovery of the polymers. In the laboratory, PHA can be obtained with high purity and yield, but most methods employed are undesirable at the industry level. PHA is usually extracted from the cells and purified through the use of organic solvents, such as chloroform, or using enzymatic or chemical cell wall disruption methods, which impair their large scale production due to economic and environmental reasons [23, 25].

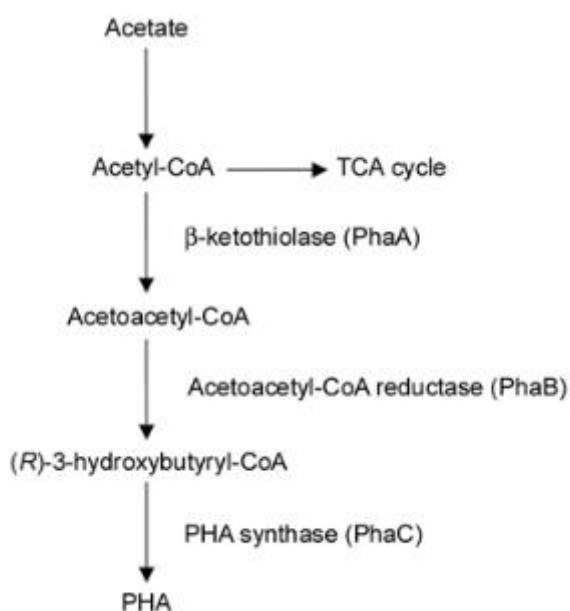


Figure 1.2. Simplified PHA biosynthesis metabolic pathway.
Adapted from Kunasundari et al. [23].

1.2. Polysaccharide Gels

Some hydrophilic polymers, such as polysaccharides, have the ability to form hydrogels under specific conditions. Hydrogels are polymeric structures composed of water-swollen polymers, with varying degrees of cross-links [29], whose network may contain up to thousands of times the weight of the dry polymer [30].

Hydrogels may be classified in multiple ways. As to their network structure, hydrogels may be classified as permanent/chemical gels, or reversible/physical gels. Permanent gels are those in which the network structure is made by covalent bonding of the cross-links and are usually not homogenous as different sites of the gel may contain more or less cross-links (and therefore less or more water particles, respectively). Reversible gels are held together by the action of secondary forces, such as ionic, hydrogen or hydrophobic forces, as well as molecular entanglements, the latter of which contributes to a non-homogenous gel [30]. When these gels are formed by the action of a multivalent ion of opposite charge of the polymer, an ionotropic hydrogel is formed. The stability of ionotropic hydrogels is very dependent on several factors, such as the valency of the ion used, which will determine the cross-links in the gel, as well as the concentrations of the polyelectrolyte and the multivalent ion. Furthermore, environmental conditions play an important role regarding the use of these gels, as the reversible bonds can be easily broken by changes in the physical conditions of the medium such as ionic strength, pH, temperature, pressure or solute competition [30].

Other methods of classification of gels exist, such as the number of different components in the gel matrix (simple, composed of a single component such as a polysaccharide; mixed, composed of two or more components such as two polysaccharides; or composites, in which the matrix is composed of two or more different components, such as a polysaccharide and a protein) or by the gelation procedure involved, including cold-set, heat-set, ionotropic, pH, or enzyme induced gelation methods [31].

1.2.1. Gel Particles

Smaller sized particles (micro and nano) have been increasingly studied due to the different interesting properties shown when particles reach such scales, especially at nano-scale where size-dependent properties really come into play, as surface/volume ratio largely increases [32]. Biopolymers have been investigated to develop these novel sized structures (beads, spheres and capsules), in which different compounds could be encapsulated, including antioxidants, vitamins, pre- and probiotics for food applications [33], but also pharmaceuticals for the medical field [34].

The preparation of such particles should include the use of non-toxic solvents, be economically feasible and account for the properties desired for the matrix, including particle size and shape, surface charge and permeability to the encapsulated components. Various methods for the preparation of polymeric particles are currently used, including emulsification (blending two immiscible

liquids through agitation), extrusion (dropwise addition of a polymeric solution into an ionic solution), spray drying (hot air spraying of a solution for quick solvent evaporation), coacervation (electrostatic interaction of opposite charged biopolymers) and precipitation (based on a varying capacity of the solution to solubilize the biopolymer, using two solutions with different solubilization capacities for the polymer) [34].

1.3. Polymeric Films

Polymeric films are thin layers of a polymeric material or blend of materials [35]. Natural polymer films have been reported for their good mechanic or barrier properties and were proposed to be used in the food industry (in applications such as packaging) or the medical field (as topic drug delivery and wound healing systems). Such polymeric films are usually easy to manufacture, cost-effective and biocompatible, and sometimes display adhesive properties [36].

Regarding porous cell scaffolds for the medical field, several methodologies for film formation have been described, including solution casting and solvent evaporation, and particle leaching (consisting of a dissolved polymer with insoluble particles suspended on that specific solvent being cast on a surface for the evaporation of the solvent, and then washed with a different solvent to remove the particles) or emulsion freeze-drying (in which an emulsion of two immiscible liquids, one of which contains the dissolved polymer, is freeze-dried) [37]. Other techniques include gas foaming (in which a salt is used to release gas particles into the medium under certain conditions, such as temperature, followed by freeze drying) or 3D-printing of the scaffold (using CAD designs) [37, 38]. Among porous films for biological uses, PHA films (PHB and PHBHV) have been investigated and reported as suitable for constructing *in vitro* matrices [39]. Furthermore, PHB and copolymeric P(3-HB-co-4-HB) have been successfully blended with a polysaccharide (bacterial cellulose, BC) and the respective blends (PHB-BC and P(3-HB-co-4-HB)-BC) have been tested in fibroblasts. The results show that the polyester-polysaccharide blends produce much better porous matrices for cell adhesion, increasing the number of adherent cells when compared to the polyester films alone [40, 41].

1.4. Motivation

As mentioned above, various polymeric structures have been proposed for the medical and pharmaceutical fields and were proven quite adept to be used as drug delivery systems or tissue regenerating scaffolds. Among such structures, polysaccharide gel particles and polymeric films stand out [34, 36]. Mannans are hydrophilic and biocompatible components, with proven interesting properties such as immunomodulator, antimicrobial, antiviral, antioxidant, antimutagenic and antitumor activity [3, 14, 15]. PHAs are biocompatible polymers with diverse possible arrangements and interesting physical and thermal properties, comparable to those of commercially available polymers [23, 24].

Nevertheless, any polymer proposed for biological applications must be individually submitted to extensive and thorough tests, to evaluate its biocompatibility and cytotoxicity. *In vitro* tests are essential and determinative forefront tests than must be performed to assess a material's biological compatibility. They represent the frontline safety barrier for compounds to reach human (and animal) applications, and though they are not representative of complete systems (such as organs or the full body), *in vitro* tests grant researchers relevant insights on how compounds will affect their targets *in vivo*. As such, a proper choice of the cell models and the employed methodologies must be made in order for *in vitro* tests to be representative.

As such, the objective of this thesis was to produce and extract these polymers from their producing organisms (mannans from the cell-wall of the yeast *Komagataella pastoris* and PHAs from the biomass of a mixed microbial culture) and use them to create different structures for biological applications. Mannans were tested for their gelling capacity and used to manufacture different gel particles using di- and trivalent cations following ionotropic gelation procedures. The produced gel particles were tested with different tumoral cell lines and a regular skin fibroblast cell line, in order to be potentially used as a drug delivery system for cancer. PHAs and mannans were used to produce polymeric films (both alone and blended) and their cytotoxicity and capacity to support cell adherence was determined using normal fibroblasts and a tumoral cell line, envisaging their use as drug delivery systems or wound dressings.

Chapter 2. Materials and Methods

2.1. Polysaccharide

2.1.1. Polysaccharide Production

2.1.1.1. Inoculum Preparation

Komagataella pastoris (DSM 70877) was used to produce the polysaccharide in use, mannans. The yeast was cultivated in medium K, with the following composition: KH_2PO_4 , 28 g L⁻¹; $\text{CaSO}_4 \cdot 2\text{H}_2\text{O}$, 0.125 g L⁻¹; $\text{MgSO}_4 \cdot 7\text{H}_2\text{O}$, 2 g L⁻¹; $(\text{NH}_4)_2\text{SO}_4$, 13.5 g L⁻¹. Medium K was supplemented with 2 mL L⁻¹ of a trace mineral solution, with the following composition: $\text{CuSO}_4 \cdot 5\text{H}_2\text{O}$, 2 g L⁻¹; $\text{MnSO}_4 \cdot \text{H}_2\text{O}$, 3 g L⁻¹; ZnCl_2 , 7 g L⁻¹; $\text{FeSO}_4 \cdot 7\text{H}_2\text{O}$, 22 g L⁻¹; Biotin, 0.2 g L⁻¹; H_2SO_4 , 5 mL L⁻¹. The pH was adjusted to 5.0 with NaOH 2 M.

The inoculum was prepared in four 500 mL shake flasks, adding 1 mL of cryopreserved yeast to each of them holding 200 mL of medium K supplemented with 45 g L⁻¹ glycerol (Scharlau, 86-88 % w/w). The inoculum was incubated for 40 h at 30 °C and 200 rpm in an orbital shaker (IKA KS 260 basic).

Medium K and glycerol were sterilized separately by autoclaving (Uniclave 77, Portugal) at 121 °C for 20 min, and the trace mineral solution was sterilized by filtration (Whatman, 0.2 µm).

2.1.1.2. Bioreactor Assay

The production assay was performed in a 10 L bioreactor (BioStat B-plus, Sartorius), with a starting volume of 8 L, using medium K prepared as described above (2.1.1.1.1.). The inoculum was added in a 10 % (v/v) ratio to the bioreactor.

The culture was grown in batch mode until the depletion of the carbon source (at around 24 h), at which point a fed-batch phase was initiated and kept for the remainder of the assay (26 h). For the fed-batch phase, 3430 g of glycerol were used, supplemented with 67 mL of trace mineral solution, at a constant flow of 144.64 g h⁻¹. The assay was conducted with controlled temperature (30 ± 0.1 °C), as well as controlled pH (5.0 ± 0.02), through the addition of either HCl 2 M or NH_4OH 25 % (v/v). The dissolved oxygen concentration (pO_2 , %) was controlled by the automatic adjustment of the stirring (between 300 and 1500 rpm) by two six-blade impellers. The setpoint was 15 % of the air saturation.

Periodic samples (10 mL) were retrieved from the bioreactor for biomass quantification.

2.1.1.3. Analytical Techniques

2.1.1.3.1. Cell Growth

Cell growth was monitored during the experiment by measuring the optical density at 600 nm ($\text{OD}_{600\text{nm}}$) in a UV-Vis spectrometer (VWR V-1200). The absorbance of the samples was kept under

0.3 by dilution of the broth with deionized water.

2.1.1.3.2. Biomass Quantification

Biomass quantification was performed gravimetrically. The cell dry weight (CDW) was determined by treatment of the acquired samples, namely by centrifugation (Sigma, 4-16KS) at 8875 g for 15 min at 4 °C to remove the supernatant, and subsequent washing of the pellet with deionized water. The washed biomass was afterwards deep frozen (-80 °C) and freeze dried (Telstar, Cryodos) for 48 h at -90 °C. The CDW was defined by the resulting weight of the lyophilized pellet.

2.1.2. Polysaccharide Extraction and Purification

NaOH 2 M was added in a 1:1 (v/v) ratio to the culture broth for an alkali-heat treatment, as previously described by Freitas and co-workers [42]. The resulting mixture was heated up to 65 °C, for 2 h under constant stirring (400 rpm). After cooling, the mixture was subjected to centrifugation (13131 g, 15 min, 4 °C) for separation of cell-wall polymers.

Mannans were recovered from the supernatant (alkali soluble fraction) and dialyzed with a 12000 MWCO membrane against deionized water at room temperature (20 °C) for 48 h. The dialysis was performed under regular water exchanges accompanied by pH and conductivity measurements, being stopped at neutral pH (between 6.0 and 7.0) and low conductivity ($< 50 \mu\text{S cm}^{-1}$). The resulting dialyzed polymer was then freeze dried (Telstar, Cryodos) for 48 h at -90 °C. The polymer was kept in closed sample containers (30 mL) with screw caps, at room temperature and sheltered from light and moisture until use.

2.1.3. Polysaccharide Characterization

2.1.3.1. Monomeric Analysis

Mannans were analyzed regarding their monomeric composition. Briefly, 5 mg of polymer were digested with 2 % trifluoroacetic acid (Sigma-Aldrich, 99 %) in deionized water at 120 °C for 2 h. The resulting hydrolysate was diluted (1:5 v/v in deionized water) and filtered (0.2 μm nylon membrane, VWR) for high pressure liquid chromatography (HPLC).

HPLC analysis was conducted using a CarboPac PA10 4x250 mm + Aminotrap column (Dionex) equipped with an amperometric detector, using NaOH 18 mM at 1 mL min⁻¹ as eluent, at 25 °C. Glucose (Fisher Scientific, 99.5 %), mannose (Sigma-Aldrich, 99.0 %) and glucosamine (Sigma-Aldrich, 99.9 %) were used as standards in ultrapure water ranging from 1 to 100 $\mu\text{g mL}^{-1}$, covering the concentrations of monomer contents of the mannans samples.

2.1.3.2. Protein Quantification

Protein content of the samples was determined by a protein precipitation method, using trichloroacetic acid (TCA) (Scharlau, 99.5 %). A mixture of 1 g of polysaccharide with 2 g of TCA was made in ultrapure water, and the solution was left at 4 °C for 15 min. After the settling period, it was centrifuged (7155 g, 15 min, 4 °C) and the protein pellet was separated from the supernatant. The supernatant was submitted to the same process until there was no visible pellet formation, after which it was dialyzed by the process described above (2.1.1.2.). The various pellets were put together as one, repeatedly washed with deionized water, and both pellet and supernatant were freeze dried as described in section 2.1.1.2. and sent for elemental analysis. Precipitated protein was quantified gravimetrically from the precipitation pellet, and total protein was estimated based on a 6.25 factor of total nitrogen found in the sample, a non-specific factor developed by Jones [43].

2.1.3.3. Moisture Content

The moisture content of the polysaccharide was measured gravimetrically, by leaving a predetermined amount of mannans to dry in an oven (100 °C) overnight. The polymer weight was then measured and left in open air until constant weight (48 h).

2.1.3.4. Inorganic Content

Mannans inorganic content was determined gravimetrically, by placing a predetermined amount of polymer (50 mg), previously dried at 100 °C for water removal, in an oven (Nabertherm, LE060K1BN Compact Muffle Furnace) at 500 °C overnight. The resulting powder was then weighted. The assay was done in triplicate.

2.1.3.5. Elemental Analysis

For elemental analysis, a predetermined amount of polysaccharide was delivered as obtained from the purification step. Elemental analysis was performed regarding nitrogen, carbon, hydrogen and sulfur using an Elemental Analyzer (Thermo Finnigan-CE Instruments, Flash EA 1112 CHNS Series), using a Multiseparation Column (SS; 2 m; 6x5 mm). Combustion reactor temperature was of 950 °C and sulfanilamide was used as standard, with a composition of 16.26 % N, 41.85 % C, 4.68 % H e 18.62 % S, using factor K as calibration.

2.1.3.6. Phosphate Content

Phosphate was analyzed by Inductively Coupled Plasma Atomic Emission Spectroscopy (ICP-AES).

Samples were prepared by diluting the polysaccharide (10 mg ml⁻¹) and were then sent for analysis. Analysis was performed using an ICP (Ultima model, Horiba Jobin-Yvon, France) equipped with a 40.68 MHz RF generator and a Czemy-Turner sequential monochromator with 1.00 m and a nebulizer (MiraMist). Phosphorus Standard for ICP 1000 mg L⁻¹ (Sigma-Aldrich, Trace-CERT) was used as standard, diluted in ultrapure water ranging from 1 to 100 mg L⁻¹.

2.1.4. Polysaccharide Transformation

2.1.4.1. Deproteination

Deproteinized mannans were obtained using the protein quantification method described above (2.1.1.3.2.), by recovery of the protein-free supernatant followed by dialysis using a 12000 MWCO membrane (20 °C, 48 h) and freeze drying (-90 °C, 48 h). The polymer was kept in closed sample containers (30 mL) with screw caps, at room temperature and sheltered from light and moisture until use.

2.1.4.2. Phosphorylation

A phosphorylation procedure, adapted from DiLuzio [44], was applied to mannans, in an attempt to increase mannans content in phosphorous. Briefly, 1 g of mannans was dissolved in 50 mL DMSO and heated up to 100 °C, at which point 10 mL of orthophosphoric acid (H₃PO₄, Sigma-Aldrich, 85 %) were added dropwise, under constant magnetic stirring (400 rpm). The temperature of the reaction was maintained for 6 h, after which the solution was allowed to cool at room temperature. After cooling, it was dialyzed using a 12000 MWCO membrane (20 °C, 48 h) and freeze dried (-90 °C, 48 h) to obtain the phosphorylated polymer. The polymer was kept in closed sample containers (30 mL) with screw caps, at room temperature and sheltered from light and moisture until use.

2.2. Polyester

2.2.1. Polyester Extraction and Purification

Polyesters, namely polyhydroxyalkanoates (PHAs), were extracted from previously produced mixed cultures dry biomass. Biomass with accumulated PHA was provided by Mariana Matos and Liane Meneses from the BioEng group. PHA production occurred in a three-step process: a first step consisting in the acidogenic fermentation of a fruit waste pulp (supplied by SumolCompal SA, Portugal) into organic acids and ethanol, used as carbon source for the production of PHAs; a second step consisting of a Feast and Famine feeding mode to select PHA accumulating bacteria; and a third step, where the selected microorganisms were fed the resulting carbon source from the acidogenic fermentation process in a pulse feeding mode (controlled by DO), under limiting nitrogen conditions to impair cell growth [28]. The third step was conducted in a 10 L bioreactor for the production of PHA

with 17 % HV content, and in 50 L bioreactors for the production of PHAs with 18, 27 and 38 % HV contents.

The extractions occurred using a Soxhlet extractor (250 mL extractor, Lenz-Laborglasinstrumente), in which a biomass filled cartridge (working as a thimble) was placed inside the main chamber of the apparatus (holding 5 g of dry biomass), and chloroform (Honeywell, 99.4 %) was used as solvent (250 mL). The extraction period was of 24 h at 90 °C. After the extraction, the solution was recovered, containing both the polyester and membrane lipids dissolved in chloroform. The purification process consisted of pouring the solution dropwise in glacial ethanol (Carlo Erba, 99.9 %) in a 10 % (v/v) ratio to remove the lipidic fraction of the sample. Lipids dissolved in ethanol, while the polyester turned insoluble and precipitated. The extraction solvent/ethanol mixture was submitted to repeating freeze-thaw cycles (-20 °C for 4 h) to ensure maximum precipitation of polyester. The polymer was then removed from the mixture and left to dry inside the fume hood at room temperature. PHAs with different compositions were obtained, namely co-polymers of 3-hydroxybutyrate (HB) and 3-hydrovalerate (HV) with varying HV contents (ranging from 17 % HV to 56 % HV).

2.3. Biopolymer Matrices

2.3.1. Gelation Procedures

Gelation procedures were tested using mannans. In a preliminary phase, it was tested the effect of pH, temperature and salt addition, in various crossed experiments. Individual mannans solutions (50 mg mL⁻¹) were submitted to different pH values (1.9, 5.6 and 9.6) at 4 °C for 96 h, as well as pH 5.6 at autoclave temperature (121 °C) for 20 min, followed by 96 h at 4 °C. In a secondary experiment, different salts were added to fresh mannans solutions (50 mg mL⁻¹) at the three tested pH values, namely FeCl₂·4H₂O (Sigma-Aldrich, 99.0 %), CuCl₂·2H₂O (Sigma-Aldrich, 99.0 %) and CaCl₂ (PanReac AppliChem, 95 %) at 20 mg mL⁻¹, and the solutions were kept at 4 °C for 72 h.

In a second phase, fresh mannans solutions (10 % (w/w)) were set at pH 5.5, 7.4, 9.4 and 11.4, and for each pH different concentrations (from 10 to 50 mg mL⁻¹) of the previously used salts were tested. Samples were kept at 4 °C and evaluated periodically over 144 h.

In both phases, mannans solutions were prepared using deionized water and the pH was set using either HCl 2 M (Fischer Scientific, 37 %) or NaOH 2 M (EKA, 97 %).

The third phase of the gelation procedures was the obtainment of gel structures. Six different versions of this experiment were performed, using either CuSO₄·5H₂O (Riedel-de Haën, 99.0 %) or FeCl₃·6H₂O (Sigma-Aldrich, 98.0 %), as follows:

- 1) Dropwise addition of mannans solution (10 % (w/w) in H₂O) to a CuSO₄ 50 mg mL⁻¹ solution;
- 2) Dropwise addition of mannans solution (10 % (w/w) in H₂O) to a FeCl₃ 50 mg mL⁻¹ solution;

- 3) Dropwise addition of mannans (10 % (w/w) in H₂O) and CuSO₄ 50 mg mL⁻¹ solution to a NaOH 2 M solution;
- 4) Dropwise addition of mannans (10 % (w/w) in H₂O) and FeCl₃ 50 mg mL⁻¹ solution to a NaOH 2 M solution;
- 5) Dropwise addition of mannans solution (10 % (w/w) in NaOH 2 M) to a CuSO₄ 50 mg mL⁻¹ solution;
- 6) Dropwise addition of mannans solution (10 % (w/w) in NaOH 2 M) to a FeCl₃ 50 mg mL⁻¹ solution.

The dropwise addition of the mannans solution (1 mL) was made using sterile needles (HenkeSassWolf, Fine-Ject, 23 G – 0.6 x 25 mm) into 30 ml of the cation solution. The structures obtained were left under stirring for 30 min and were then washed using deionized water (30 mL) for removal of excess salt and lowering of the pH value, controlled by measurement of pH (until neutral pH) and conductivity (until below 50 μ S cm⁻¹). The structures were then freeze dried (-90 °C, 48 h) and weighted. Version 4 was also repeated twice, in which the washing process was changed to either centrifugation (7155 g, 10 min, 4 °C) or dialysis against deionized water (20 °C, 24 h). In either case, the structures were then freeze dried (-90 °C, 48 h) and weighted.

2.3.2. Film Formation Procedures

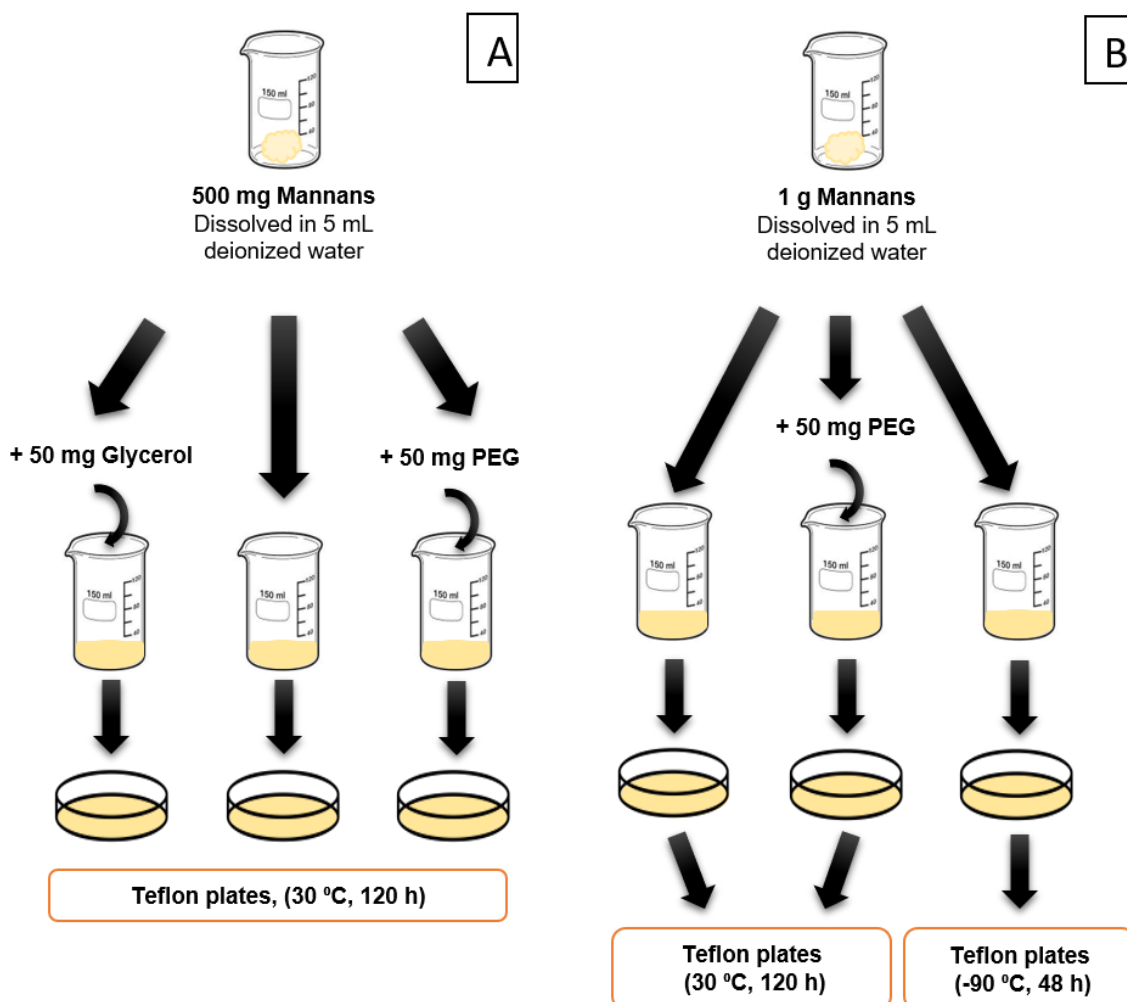
For preparation of mannans films, 500 mg of the polymer were dissolved in 5 mL of deionized water, at room temperature, under magnetic stirring (300 rpm) until complete dissolution. Two other variants of the above were performed, one to which 50 mg of glycerol (Scharlau, 86-88% w/w) were added, and another to which 50 mg of polyethylene glycol 4000 (PEG) (Fluka, Sigma-Aldrich) were added. These two components were used as plasticizers, to account for the natural brittleness of the polymeric films. The solutions were cast on Teflon plates (50 mm), and the solvent was left to evaporate in an oven (Raypa) at 30 °C for 120 h (figure 2.1 A).

In a second stage, 1 g of mannans was dissolved in 5 mL of deionized water, at room temperature, under magnetic stirring (300 rpm). This procedure was repeated, with the addition of 50 mg PEG, and both films were left to dry in an oven (Raypa) at 30 °C for 120 h. A third variant was performed as was the first (1 g mannans in 5 mL deionized water) but was instead freeze dried (-90 °C, 48 h) (figure 2.1 B). The first and the third variant of this assay were reproduced in plastic petri dish scale (Labbox, 90 mm diameter) as well as cell culture plates (VWR, 35 mm diameter) at 10 % (w/w). The first variant (petri dish) was then used to mimic some procedures developed for gelation purposes. One piece of film was placed in a FeCl₃ 50 mg mL⁻¹ solution for 2 h, and then relocated to a NaOH 2 M solution for 2 h. Another piece was placed in a FeCl₃ 50 mg mL⁻¹ solution for 2 h, and the final piece was placed inside a NaOH 2 M solution for 2 h. All three pieces of film were later washed with deionized water to

either lower pH (up until neutral pH) and/or conductivity (below $30 \mu\text{S cm}^{-1}$) (figure 2.1 C).

Also, films performed using iron gelling structures (2.2.1, version 4) dried in cell culture plates (both in an oven at 30°C and by freeze drying at -90°C for 48 h) were obtained (figure 2.1 D).

A comprehensive scheme regarding mannans films is presented in figure 2.1.





D

16

2.4. Cell Cultures

Three adherent cell lines (colorectal carcinoma cell line – HCT116; ovarian carcinoma cell line – A2780; normal human skin fibroblasts) were purchased from American Type Culture Collection (ATCC®), and one adherent cell line (modified breast adenocarcinoma cell line – MCF7-GFP) was purchased from Cell Biolabs Inc (San Diego, CA, USA). HCT116 and normal fibroblasts were grown in Dulbecco's Modified Eagle Medium (DMEM) (Gibco, Life Technologies, USA), supplemented with 10 % (v/v) FBS (Gibco, Life Technologies, USA) and 1 % (v/v) antibiotic/antimycotic solution (Invitrogen). MCF7-GFP was grown in DMEM (as above) supplemented with an additional 1 % (v/v) MEM non-essential amino acids (Gibco, Life Technologies, USA). A2780 was grown in Roswell Park Memorial Institute (RPMI) medium (Gibco, Life Technologies, USA) supplemented with 10 % (v/v) FBS and 2 mM glutamine. All cultures were maintained in an incubator (SANYO, CO₂ Incubator, Electrical Biomedical CO., Osaka, Japan) at 37 °C, with an atmosphere of 5 % (v/v) CO₂ and 99 % (v/v) relative humidity (RH).

2.5. Cytotoxicity Assays

Cytotoxicity assays were performed for both mannans and its deproteinized version, in HCT116, A2780 and normal fibroblasts. The three cell lines were independently seeded in 96-well plates (VWR, Radnor, Pennsylvania, USA) at a density of 0.75×10^5 cells per well and left to adhere for 24 h in an incubator at the conditions described above. After 24 h, seeding medium was replaced with fresh medium containing either regular or deproteinized mannans ($0 - 2000 \mu\text{g mL}^{-1}$) or control components ($0.4 \mu\text{M}$ of doxorubicin (DOX), $0.4 \mu\text{M}$ of dimethyl sulfoxide (DMSO), TCA 0.5 % (w/v)) and left for 48 h in the same conditions. After 48 h, both polysaccharide and control loaded media were replaced with fresh medium containing 20 % (v/v) Cell Titer 96® Aqueous Non-Radioactive Cell Proliferation Assay Kit (Promega, Madison, USA) (composed by 3-(4,5-Dimethylthiazol-2-yl)-5-(3-carboxymethoxyphenyl)-2-(4-sulfophenyl)-2H-tetrazolium (MTS inner salt) and phenazinemethosulfate (PMS, coupling reagent)). After a new incubation for 45 min (under the conditions described above), absorbance measurement at 490 nm was performed for each well using Tecan Infinite F200 Microplate Reader (Tecan, Männedorf, Switzerland). Cell viability (%) is given by (Eq. 1):

Eq.1

$$\text{cell viability (\%)} = \frac{Abs_{\text{cells submitted to compound}} - Abs_{\text{blank well (no cell control)}}}{Abs_{\text{medium control with cells}}} \times 100$$

A cell density of 0.75×10^5 cells per well was achieved by Trypan Blue Exclusion method. Cells were centrifuged at 500 g and resuspended in 1 mL of appropriate medium, followed by dilution to 10 % (v/v) alongside Trypan Blue reagent (Sigma, St. Louis, USA) 20 % (v/v) in the same growth medium. This solution was inserted in a hemocytometer (Hirschmann, Eberstadt, Germany), and cell count was performed by microscopic observation of viable cells using an Olympus CXX41 inverted microscope (Tokyo, Japan). Cell density (cells mL⁻¹) is given by (Eq. 2):

Eq. 2

$$cell\ density = \frac{cell\ count_{(9\ quadrants)}}{9\ (quadrants)} \times 10\ (dilution\ factor) \times 10^4\ (quadrant\ volume)$$

2.6. Cell Adherence Assays

Cell adherence assays were performed for previously described films using either normal skin fibroblasts or MCF7-GFP. Cell line MCF7-GFP was used due to microscopic observation constraints when using normal skin fibroblasts, as the films opacity cloaked the visualization of these cells. MCF7-GFP produces Green Fluorescent Protein (GFP), whose fluorescence was used to overcome the visualization constraints. Mannans films (regular mannans films (dried at 30 °C or freeze dried), iron gelling structure films (dried at 30 °C or freeze dried), and films obtained from manipulation of mannans film to mimic gelation procedure methods (first and second pieces, both dried at 30 °C)) were tested using regular fibroblasts. These films were prepared inside the cell culture plates (VWR, 35 mm), and sterilized using UV light for 30 min. A cell suspension of 0.75×10^5 cells mL⁻¹ was prepared and added to the films (1 mL per plate) and incubated for 24 h (at 37 °C, 5 % (v/v) CO₂, 99 % (v/v) RH) for cell adhesion. After 24 h, cell adhesion was verified using a fluorescence inverted microscope (Nikon Eclipse Ti), (Nikon, Intensilight C-HGFI).

PHA/mannans films were tested using both skin fibroblasts and MCF7-GFP. These films were prepared in separate glass vessels, sterilized in autoclave (121 °C, 30 min) and inserted in cell culture plates. The following procedure was identical to that used for mannans films.

Cell viability assays were also performed with pure PHA films on adherent cells. MCF7-GFP were seeded on top of pure PHA films in cell culture plates (VWR, 35 mm) at a density of 0.75×10^5 cells per plate, and incubated for 48 h at 37 °C, with an atmosphere of 5 % (v/v) CO₂ and 99 % (v/v) RH. After the 48 h incubation period, seeding medium was replaced with fresh medium containing 15 % (v/v) Cell Titer 96 ® AQueous Non-Radioactive Cell Proliferation Assay Kit (Promega, Madison, USA), and subsequently incubated for 1 h at the same conditions, after which absorbance measurement at 490 nm was performed for each plate using Tecan Infinite F200 Microplate Reader (Tecan, Männedorf, Switzerland).

Chapter 3. Results and Discussion

3.1. Polysaccharide Production

The bioreactor was operated in batch mode for the first 24 h, after which it was switched to a fed-batch mode for the remainder of the assay. Carbon source for the fed-batch mode was supplied at a constant rate of 116.84 mL h^{-1} (144.64 g h^{-1}). During the exponential phase, yeast biomass grew at a specific cell growth rate of 0.17 h^{-1} similar to that found in literature for *Komagataella pastoris* grown in glycerol by Roca and co-workers [11], reaching a maximum CDW value of 166.88 g L^{-1} at 50 h of cultivation (Figure 3.1).

Mannans content was determined to be 37.75 % (w/w) of CDW and the volumetric productivity was calculated to be $1.25 \text{ g L}^{-1} \text{ h}^{-1}$. The growth yield was $0.42 \text{ g}_{\text{biomass}} \text{ g}_{\text{glycerol}}^{-1}$, lower than that described for pure glycerol, $0.55 \text{ g}_{\text{biomass}} \text{ g}_{\text{glycerol}}^{-1}$ as described by Roca and co-workers [11]. This discrepancy could be due to glycerol that was administered to the bioreactor but which ended up not being consumed by the yeast. However, since glycerol was not quantified at the end of the assay, this hypothesis cannot be confirmed. The product yield was of $0.13 \text{ g}_{\text{mannans}} \text{ g}_{\text{glycerol}}^{-1}$.

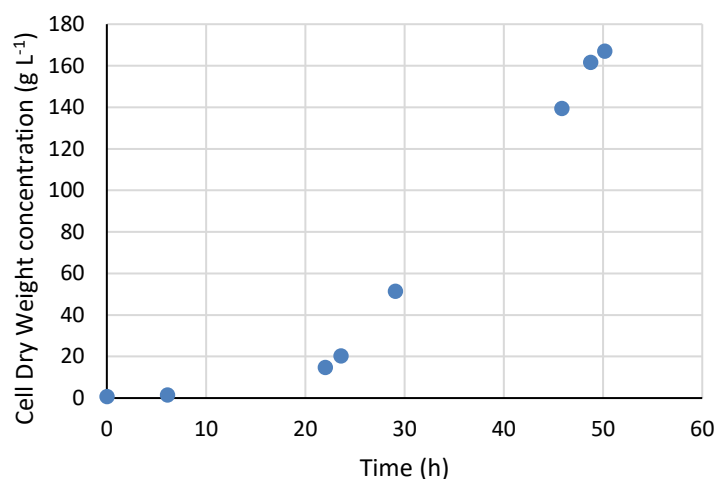


Figure 3.1. Cell Dry Weight over the course of the bioreactor assay.

3.2. Polysaccharide Characterization

3.2.1. Monomeric Analysis

Monomeric analysis of the produced mannans revealed a mannose content of $24.13 \pm 2.04 \text{ \% w/w}$. Traces of glucose ($2.27 \pm 0.02 \text{ \% w/w}$) and glucosamine ($0.78 \pm 0.01 \text{ \% w/w}$) were also detected. Glucosamine is a characteristic monomer of CGC and the fact that it was present in the sample could be proof that the extraction process was not 100 % effective, as purified mannans should not have any trace of it. This fact misleads the calculation of true monomeric content of the sample, both by underestimating the mannose content (which should be higher) and overestimating the glucose

content (which may as well be part of the CGC fraction present in the sample).

3.2.2. Protein Quantification

Protein quantification was achieved by a protein precipitation method using TCA as a precipitation agent. The total protein precipitated was as high as 19.45 ± 0.53 % (w/w). This amount of precipitated protein, however, does not encompass all the initial protein in the sample, as discussed below (3.2.5). The precipitation process also depleted the sample of about half of its remaining polymeric content, as only 41.19 ± 1.73 % (w/w) of the initial sample was able to be retrieved, which had a mannose content of 24.13 ± 2.04 % w/w. This is most likely due to hydrolysis effect caused by the TCA, as the carbohydrate sidechains of the mannoprotein fraction of the sample were too small and therefore able to cross the pore of the dialysis membrane. It is also possible that non-mannoprotein mannans were hydrolyzed into smaller polysaccharides.

3.2.3. Moisture Content

Moisture content of the mannans sample was determined to be 5.08 % (w/w).

3.2.4. Inorganic Content

Inorganic content of the mannans sample was determined to be 1.46 ± 0.09 % (w/w).

3.2.5. Elemental Analysis

Elemental analysis was performed for mannans as obtained, deproteinized mannans as well as the deproteinization pellet. Results are displayed in table 3.1.

Table 3.1. Elemental analysis of mannans.

	Element % (w/w)			
	Nitrogen	Carbon	Hydrogen	Sulphur
Mannans	6.90 ± 0.09	43.76 ± 0.01	6.86 ± 0.28	0
Deproteinized Mannans	2.09 ± 0.02	41.42 ± 0.06	6.63 ± 0.03	0
Protein Pellet	10.98 ± 0.06	57.45 ± 0.08	8.23 ± 0.26	0.30 ± 0.03

Results are presented as Mean \pm SD (%).

The results show a total of 6.90 ± 0.09 % (w/w) nitrogen content, corresponding to a protein content of 42.71 ± 0.19 % (w/w). Protein quantification was performed based on a 6.25 factor as previously described (2.1.1.3.2).

There was a total carbon content of 43.76 ± 0.01 % (w/w) in the mannans sample.

3.2.6. Phosphate Content

Phosphate content was determined for samples of original, deproteinized and phosphorylated mannans as well as for the phosphorylation pellet. Results are shown in table 3.2.

Table 3.2. Phosphate and ammonia content of mannans.

	Phosphate % (w/w)
Mannans	1.97 ± 0.17
Deproteinized Mannans	1.31
Phosphorylated Mannans	1.04 ± 0.04
Phosphorylation Pellet	0.59

Results are presented as Mean ± SD (%).

Regarding phosphate content, analysis was performed by ICP-AES). Phosphate content was determined to be 1.97 ± 0.17 % (w/w) in the original polymer. Phosphate content was determined due to its relevant role in numerous biological processes, as phosphorylated polysaccharides (both naturally occurring and transformed) have been described to have enhanced immunocompetence, anticoagulation and antineoplastic activity [45], as well as antitumor activity [3]. The content in phosphate as also been related to its activity, both immunochemical and serological [46, 47]. The phosphate content of the mannans in this study is within range from mannans obtained from different yeasts, namely *C. albicans*, which have reported values typically ranging from 0 to 2.4 %, although higher phosphate content values have been reported, almost up to 5 %, depending on cultivation conditions [48]. Other studies on *P. holstii* showed that certain fractions of polysaccharides may be even richer in phosphate contents (from 3 to 7.4 %) [49], although the complete mannans profile may not be present. Although many reported phosphomannans contain lower amounts of phosphate than the one in this study, phosphate content is a relevant factor for the desired properties, and thus an attempt to increase it was made (3.3.2).

3.3. Polysaccharide Transformation

3.3.1. Deproteinization

As described above (3.2.2), deproteinized mannans were obtained from the supernatant of the protein precipitation method, with a yield of 41.19 ± 1.73 % (w/w) for recovered polymer and a yield of 69.49 ± 0.44 % for removed protein. From the results of elemental analysis (table 3.1), it is possible to see that the TCA precipitation method did not remove all the protein from the initial sample, but total protein precipitated was higher than the previously calculated (3.2.2), totalling 29.68 ± 0.32 % (w/w). The protein precipitation method employed, using TCA, has been described as a high yielding precipitation method, with precipitation yields above 90 % for removed protein [50], well above those described in this study. Moreover, polymer recovered in that study was higher than the one reported here, with a total loss of polymer of 19 %. This shows that the TCA method employed, while effective in removing

proteins from mannans samples, is still requiring tuning to increase protein precipitation, as well as diminish wasted polymer.

There was a total carbon content of 41.42 ± 0.06 % (w/w) in the deproteinized sample and 57.45 ± 0.08 % (w/w) in the protein pellet (table 3.1).

Phosphate content in the deproteinized polymer was of 1.31 % (w/w) (table 3.2).

3.3.2. Phosphorylation

The phosphorylation procedure applied to mannans had a final yield of 29.72 % (w/w) for recovered polymer, despite the results presented above (3.2.6, table 3.2) regarding its content in phosphate, which would render a negative yield (loss) in terms of total phosphate in the polymer, of -46.64 ± 6.63 % (w/w). The method employed in the phosphorylation of mannans was adapted from a phosphorylation procedure of glucans [44], in which the author achieved a total of 2.23 % of phosphorylation after 6 h of reaction, with a total polymer recovery between 70 and 90 %. Other authors using a similar method described a total yield for recovered polymer below that achieved in this work, of 24.8 %, and postulated that the conditions of the experiment, and the type and ratios of the reagents could account for significant yield variability [51]. A different method was reported to generate a phosphorylated polysaccharide with a phosphate content as high as 14.36 % [45].

It is clear to see the diminishing in phosphate content from the original polymer to either of the transformed polysaccharides, remarkably so to the one submitted to a phosphorylation process. Not only was the phosphorylation unsuccessful, it reduced the sample content in phosphorous, most likely due to the concentration of phosphoric acid, which ended up hydrolyzing the sample much more than it added any phosphate groups. Other causes may be related to the method itself, as it was adapted from a phosphorylation procedure of insoluble glucans, and certain modifications were made regarding the soluble nature of mannans, namely the use of urea as a chaotropic agent.

Phosphate content of the sample showed a total of 1.04 ± 0.04 % (w/w) in the phosphorylated polymer and 0.59 % (w/w) in the phosphorylation pellet.

3.4. Polyester Extraction and Purification

Different PHAs were used, with varying monomeric composition in terms of hydroxybutyrate (HB) and hydroxyvalerate (HV). The PHAs used include PHB (100 % HB monomers), PHBHV17 (83 % HB, 17 % HV), PHBHV18 (82 % HB, 18 % HV), PHBHV27 (73 % HB, 27 % HV), PHBHV38 (62 % PHB, 38 % HV) and PHBHV56 (44 % HB, 56 % HV).

All polymers except PHBHV18 were extracted with chloroform with a Soxhlet apparatus and purified by precipitation in cold ethanol. PHBHV18 was first extracted with hypochlorite (bleach) and

subsequently it was purified to remove any trace amounts of the solvent, for biological applications.

3.5. Biopolymer Matrices

3.5.1. Gelation Procedures

As previously described (2.2.1), gelation procedures were only performed using mannans. In the preliminary phase, pH and temperature were the main focus, with a small insight on salt effect. Temperature was the first variable to be refined, as gel formation only started to occur at low temperatures (4 °C). No gel formation was visible at room temperature, and at higher temperatures (121 °C) the solution resulted in a turbid, granulated precipitate upon cooling. pH was also pre-refined, as acidic pH (pH 1.9) had a negative effect in the solution (high turbidity and no gel formation) both in the presence and absence of different salts (FeCl₂, CuCl₂ and CaCl₂). Neutral and alkaline pH (pH 5.6 and 9.6) displayed a beneficial effect (increased viscosity and clearness of the solution) when combined with the different salts used. Preliminary results are displayed in tables 3.3 and 3.4.

Table 3.3. Effect of pH and temperature on mannans solutions gelation.

pH	Temperature		
	4 °C	20 °C	121 °C
1.9	-	-	n.a.
5.6	+	-	pp
9.6	+	-	n.a.

Results are displayed as (-, no gel formation; +, increased viscosity; pp, precipitate; n.a., not available/ not tested).

Table 3.4. Effect of pH and salt presence on mannans gelation at 4 °C.

pH	Salt		
	FeCl ₂	CuCl ₂	CaCl ₂
1.9	-	-	-
5.6	+	+	+
9.6	+	+	+

Results are displayed as (-, no gel formation; +, gel formation).

Salt effect was further tested using an array of different pH (both neutral and alkaline, pH 5.5, 7.4, 9.4 and 11.4) and incremental concentrations (10 mg mL⁻¹) of the three different salts (from 10 to 50 mg mL⁻¹), and were kept at 4 °C, as displayed in table 3.5 and figure 3.2. Calcium salts were deemed the most unstable, despite the fact that gel formation was still evident. This is due to the low resistance of the resulting gel to mild agitation which seemed irrespective to either pH or salt concentration used. Both iron and copper salts were considered effective in this assay, in all pH and salt concentrations tested. Notably, these were much more resistant to mild agitation and only reverted to their original state under constant agitation and temperature raise to room temperature. This reversion effect was also conditioned by the pH and salt concentration, as higher values of either these variables delayed the reversion process. Also, two distinct phases were observable in all gels formed, most likely caused by water syneresis from the gel.

Table 3.5. Effect of pH and salt concentration on mannans gelation at 4 °C.

Results are presented as (+, weak gel; ++, strong gel).

Salt Concentration (mg mL ⁻¹)	pH				pH				pH			
	5.5	7.4	9.4	11.4	5.5	7.4	9.4	11.4	5.5	7.4	9.4	11.4
10	+	+	+	+	+	+	+	+	+	+	+	+
20	+	+	+	+	+	+	+	+	+	+	+	++
30	+	+	+	+	+	+	+	++	+	+	++	++
40	+	+	+	+	+	+	++	++	+	++	++	++
50	+	+	+	+	+	+	++	++	+	++	++	++

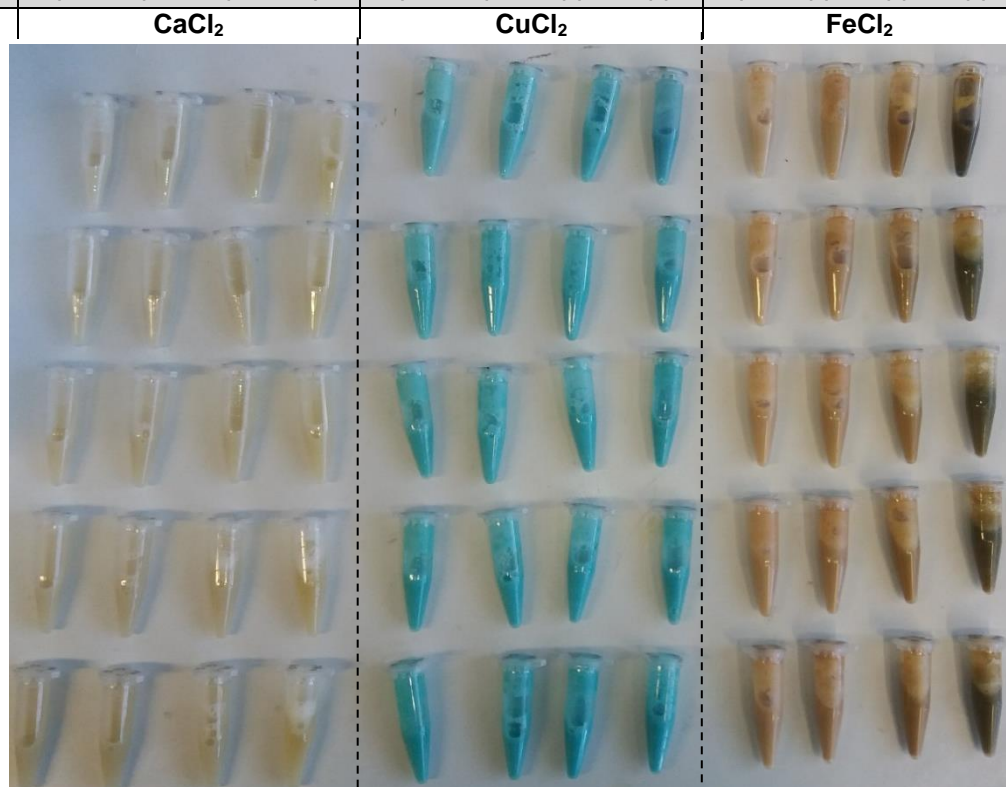


Figure 3.2. Effect of pH and salt concentration on mannans gelation at 4 °C.

The various solutions in the figure correspond, in the same order, to the entries in table 3.5 above.

After selection of temperature, pH conditions and salts to test, a new phase began regarding the formation of structured gel particles, as previously described (2.2.1), by six different versions of the same experiment. Versions differ from each other regarding the order of the addition of the components, pH and salt used, as displayed in table 3.6 alongside the main results. Images from the resulting beads are displayed in figure 3.3.

Table 3.6. Different versions employed for structured gel particles formation.

Version	Solutions in Syringe		Stirring Solution	Bead Shape	Stability		
	Sol. 1	Sol. 2			Agitation	Wash	Degradation
1	Mannans 10 % (w/w)	x	CuSO ₄ 0.2 M	Ring	--	--	--
2	Mannans 10 % (w/w)	x	FeCl ₃ 0.185 M	Ring	--	--	--
3	Mannans 10 % (w/w)	CuSO ₄ 0.2 M	NaOH 2 M	Spherical	+	--	-
4	Mannans 10 % (w/w)	FeCl ₃ 0.185 M	NaOH 2 M	Spherical	++	+	+
5	Mannans 10 % (w/w)	NaOH 2 M	CuSO ₄ 0.2 M	Spherical	--	+	+
6	Mannans 10 % (w/w)	NaOH 2 M	FeCl ₃ 0.185 M	Ring, Spherical	--	+	+

In Sol. 2 column, x means absent. Results are presented as (--, very susceptible; -, susceptible; +, resistant; ++, very resistant).

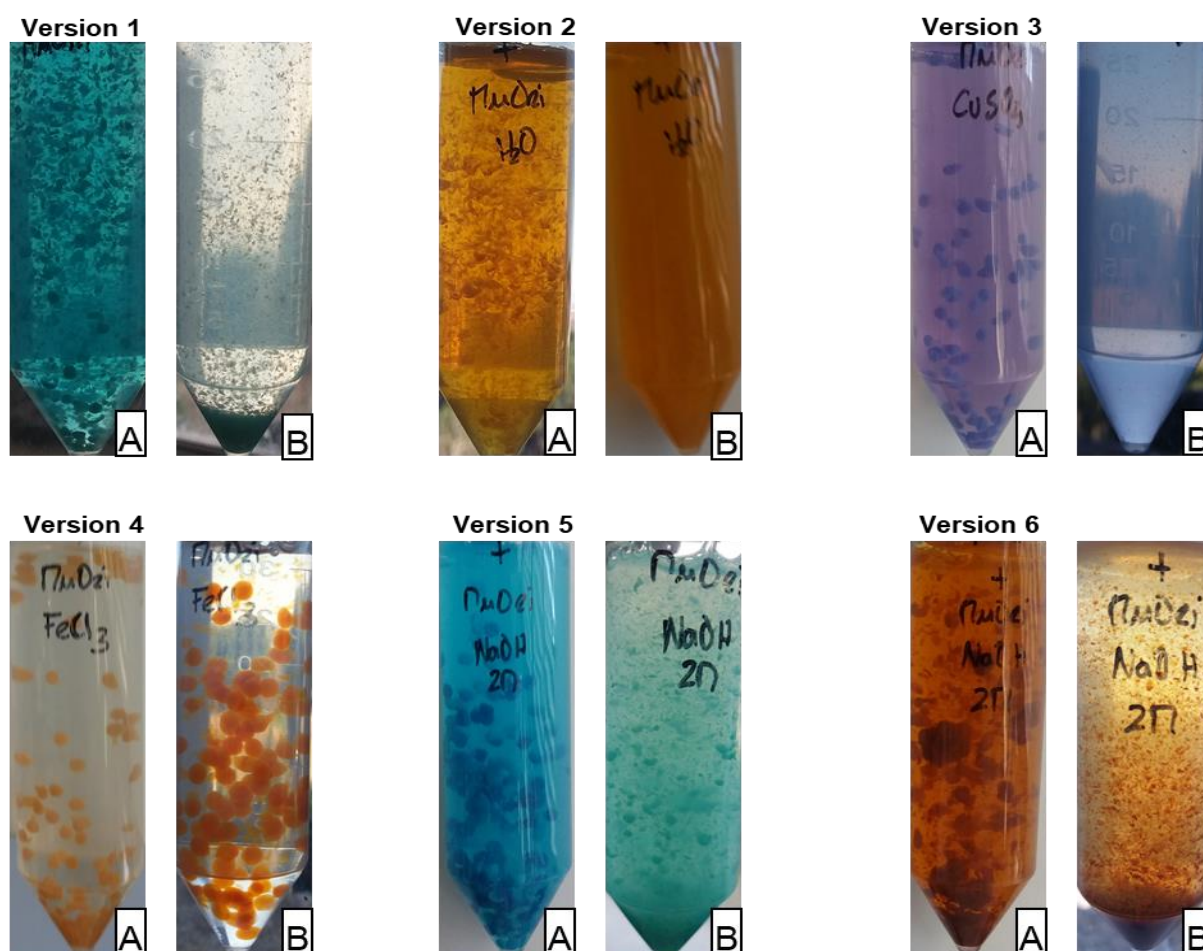


Figure 3.3. Beads resulting from different versions employed for structured gel particles formation.

(A) Beads immediately after dropwise addition (in stirring solution); (B) Beads after washing process (in deionized water). Versions are indicated on top of the respective (A) figure.

Version 1 consisted in a dropwise addition of mannans solution (10 % (w/w) in H₂O) into a CuSO₄ 0.2 M solution under stirring. The resulting structures were ring shaped (figure 3.3-1A), and very susceptible to mild agitation and washing, degrading into small insoluble particles of varying shape

and size (figure 3.3-1B).

Version 2 consisted in a dropwise addition of mannans solution (10 % (w/w) in H₂O) to a FeCl₃ 0.185 M solution. The obtained structures were ring shaped, but degraded into a polymeric cloud, devoid of any individual shape under mild agitation (figure 3.3-2A). After washing only few polymeric insoluble debris remained (figure 3.3-2B).

Version 3 consisted in a dropwise addition of mannans (10 % (w/w) in H₂O) and CuSO₄ 0.2 M solution to a NaOH 2 M solution under stirring. Structures obtained with this method were spherical and more resistant to mild agitation (figure 3.3-3A). However, as in version 1, the formed structures were susceptible to degrading during washing, yielding small insoluble particles after reaching neutral pH and low conductivity (figure 3.3-3B).

Version 4 consisted in a dropwise addition of mannans (10 % (w/w) in H₂O) and FeCl₃ 0.185 M solution to a NaOH 2 M solution. The resulting structures were spherical and much more resistant to mild agitation and washing process than any other structures (figure 3.3-4A). They retained their spherical structure with little aggregation after the washing process (figure 3.3-4B) and only started degrading after a few hours in deionized water.

Version 5 consisted in a dropwise addition of mannans solution (10 % (w/w) in NaOH 2 M) to a CuSO₄ 0.2 M solution. Structures formed were spherical but, unlike version 3, were not more resistant to mild agitation than version 1 structures (figure 3.3-5A). These were, however, more resistant to the washing process, degrading only after a few hours in deionized water (figure 3.3-5B).

Version 6 consisted in a dropwise addition of mannans solution (10 % (w/w) in NaOH 2 M) to a FeCl₃ 0.185 M solution. The structures obtained were irregular, both spherical and ring shaped (figure 3.3-6A), and degraded with mild agitation (figure 3.3-6B), yet retaining their shape for a few hours after the washing period.

These experiments evidenced the role of alkaline pH in the formation of the beads, namely their shape, as neutral pH formed ring shaped (flat) structures and alkali pH induced the formation of spherical structures. Also, the order of the addition of the components had an impact in their final stability, as a polymer and salt mixture being dropped onto a NaOH solution rendered more stable beads. Furthermore, trivalent iron seemed to have an increased effect over divalent copper in the resistance of the structured gel, as opposed to divalent iron used in the previous experiment, which displayed similar results to divalent copper.

Considering both shape and stability, version 4 of this experiment was selected, and different washing processes were attempted, aiming at reducing its impact in the time the structures lasted in deionized water (degradation). Centrifugation reduced the number of intact spheres after the washing process, yet a few were still visible, whereas dialysis degraded the spheres even before the end of the process. A simple deionized water washing was therefore deemed the most effective, and the resulting beads were placed in cell culture plates and laid aside for film formation.

3.5.2. Film Formation Procedures

3.5.2.1. Polysaccharide Films

In an early stage, mannans films were performed in deionized water (plain, with glycerol and with polyethylene glycol 4000 (PEG)), cast in Teflon plates and left to evaporate in an oven at 30 °C. Mannans films obtained in Teflon plates are displayed in figure 3.4. The plain mannans films obtained were rigid and brittle and broke into small pieces at the time of removal from the Teflon plate (figure 3.4 A). The glycerol version never fully dried and at the time of its removal from the Teflon plate it lost its integrity, forming a paste, and ended being discarded from further tests (figure 3.4 B). This paste effect could be due to the fact that glycerol is hydrophilic and has the capacity to retain water molecules inside the film, which is an important part of its plasticizer ability [52]. The PEG version was also brittle and rigid, breaking into small pieces at the time of its recovery from the Teflon plate (figure 3.4 C). Regarding the frailness of the obtained films (pure and PEG), an increase in polymer was also tested to increase the thickness of the film, but to no avail, as the results were similar (figures 3.4 D and E, respectively). Since PEG added little to no improvement to the film formation, it was discarded from further uses.

A new method was then attempted, in which mannans were dissolved in deionized water but the removal of the solvent occurred by freeze drying (-90 °C, 48 h). The film formed in this manner had a higher volume (and consequent, a higher porosity), was less frail than its previous counterpart and was successfully removed from the Teflon plate (figure 3.4 F). The mannans film formation process was repeated in two different scales, in petri dish (90 mm diameter) (figures 3.5 B and C) and in cell culture plate (35 mm diameter) (figure 3.5 A) scale, regarding both solvent removal methods, in perfectly flat surfaces (since the Teflon plates used were slightly convex, resulting in a thinner central disk of the film). The resulting films seemed unaffected by the flat nature of the plates tested, displaying similar properties to the ones obtained in Teflon plates (figure 3.5).

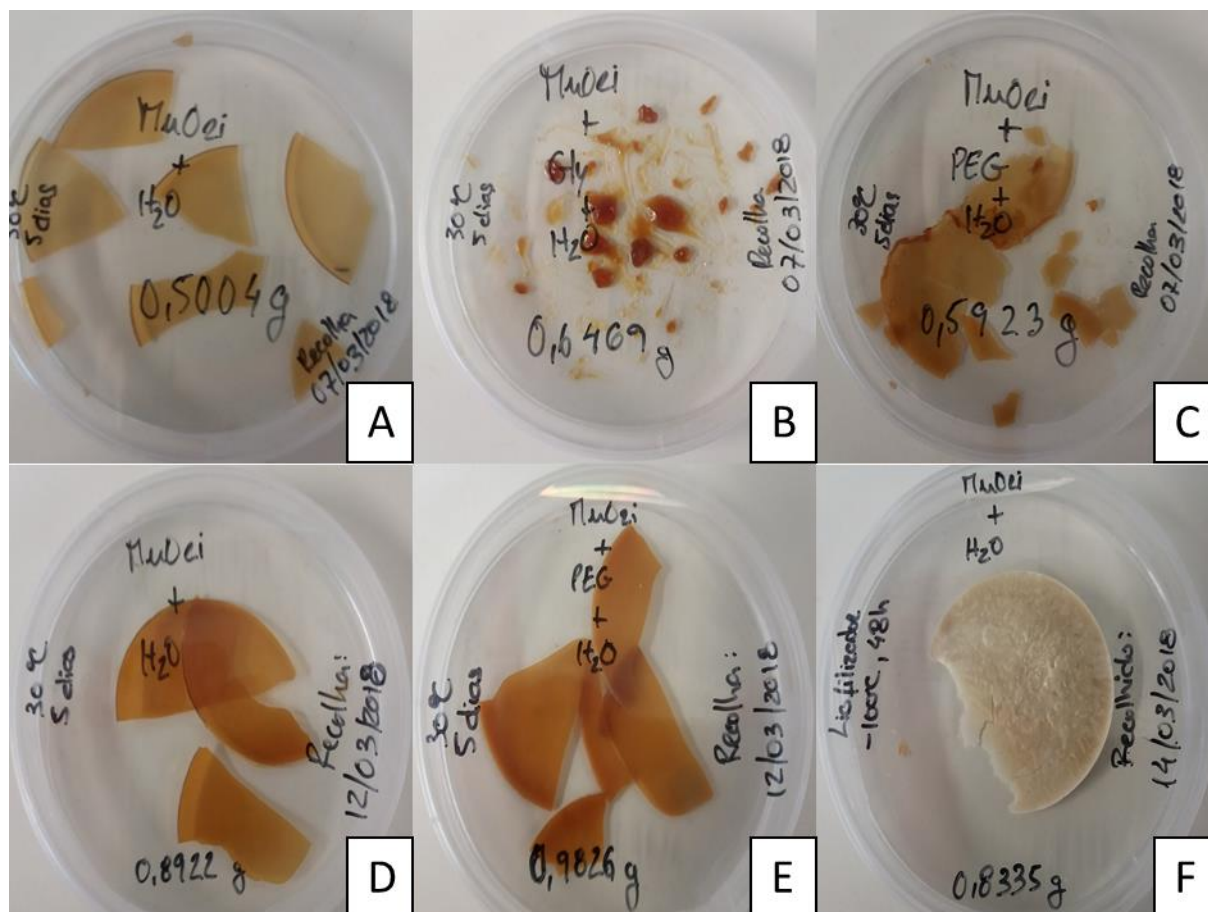


Figure 3.4. Early stage mannans films obtained in teflon plates.

(A) plain mannans film (30 °C); (B) mannans film with glycerol (30 °C); (C) mannans film with PEG (30 °C); (D) plain mannans film (higher concentration) (30 °C); (E) mannans film with PEG (higher concentrations) (30 °C); (F) plain mannans film (-90 °C).

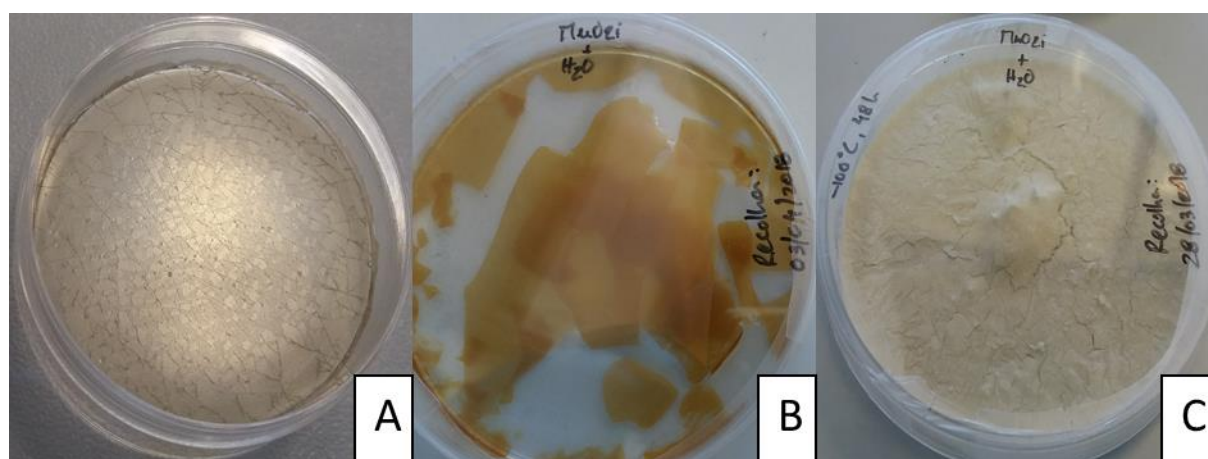


Figure 3.5. Plain mannans films obtained in petri dish and cell culture plate scale.

(A) mannans film obtained in cell culture plate (30 °C); (B) mannans film obtained in petri dish (30 °C); (C) mannans film obtained in petri dish (-90 °C).

Films obtained in the cell culture plates were laid aside for biological assays (original mannans dried in oven – MnOri30; original mannans freeze dried – MnOri-90), and the film obtained in petri dish scale (dried in oven at 30 °C) was used to mimic the gelation procedures tested (using iron salt) for bead

formation. This film was divided, and each piece suffered a different treatment, one placed in a FeCl_3 0.185 M solution for 2 h (MnOriFeFilm), another placed in a NaOH 2 M solution for 2 h, and a third piece placed in a FeCl_3 0.185 M solution for 2 h and then relocated to a NaOH 2 M solution for 2 h (MnOriFeNaOHFilm). The purpose of these treatments was to turn the mannans film insoluble, following selected procedures used to make seemingly insoluble beads. The treatments tested revolve around the version 4 procedure (3.5.1), which yielded the best results. Since the mannans film is a compact structure rather than a solution, iron and mannans could not be mixed. Instead, the film was soaked in the iron solution and then allocated to a NaOH solution. Two other treatments were employed, one similar to version 2 (3.5.1) in which the film was only immersed in the iron solution, and another in which the film was only immersed in a NaOH solution. These last two treatments were used to verify if either of the parts of the first treatment could improve the film insolubility alone. The piece placed only in NaOH 2 M dissolved completely, but the other two pieces were washed to remove excess salt and to lower pH (until neutral pH and conductivity lower than $30 \mu\text{S cm}^{-1}$), placed in cell culture plates, dried in an oven (30°C), and laid aside for biological assays.

The beads obtained by version 4 (3.5.1) were also used for film formation, by drying in an oven at 30°C (MnOriFeBeads30) or by freeze drying at -90°C for 48 h (MnOriFeBeads-90) and were laid aside for biological assays.

All mannans films hereby marked as “laid aside for biological assays” are displayed in table 3.7.

Table 3.7. Mannans films prepared for biological assays.

Films	Provenance	Drying Method
MnOri30	Cell culture plate Film	Oven (30°C)
MnOri-90	Cell culture plate Film	Freeze-Dry (-90°C , 48 h)
MnOriFeFilm	Petri dish Film + Version 2 (3.5.1)	Oven (30°C)
MnOriFeNaOHFilm	Petri dish Film + Version 4 (3.5.1)	Oven (30°C)
MnOriFeBeads30	Version 4 beads (3.5.1)	Oven (30°C)
MnOriFeBeads-90	Version 4 beads (3.5.1)	Freeze-Dry (-90°C , 48 h)

3.5.2.2. Polyester Films

The polyesters obtained were also used to prepare films. Firstly, two different methods were tested (figure 3.6), consisting of dissolving PHAs in chloroform and 1) mannans in water and mixing both solutions to form an emulsion (figure 3.6 A), or 2) suspending mannans in powder form in chloroform (figure 3.6 B). The water/chloroform method was performed to test the capacity for the formation of an emulsion between the two phases containing the different polymers. An emulsion was achieved, but the differential evaporation of the two solvents caused segregation of the polymers, and the films obtained were highly irregular and irreproducible, with mannans clustered on a side from top to bottom of the film, making them impossible to be removed whole (figure 3.6 A). However, when mannans were suspended in chloroform for film formation, solvent evaporation was uniform, and even though mannans were not dissolved, the obtained films were more evenly formed, composed of two different polymeric layers with apparent polymer segregation, but uniform layers nonetheless (figure 3.6 B).

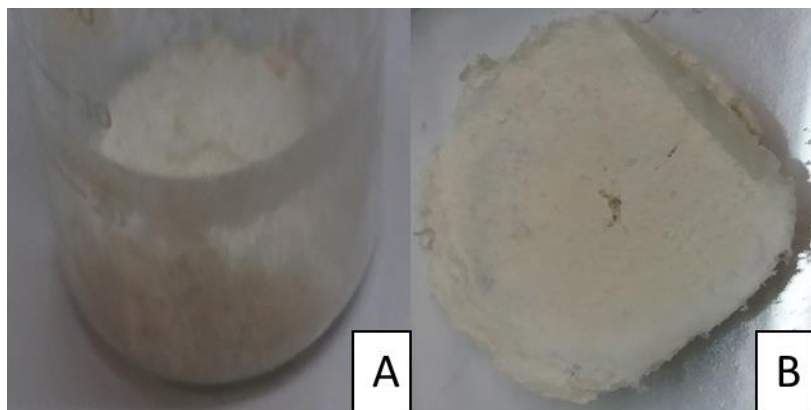


Figure 3.6. Methods for PHA/mannans films preparation.

(A) PHA dissolved in chloroform and mannans dissolved in water; (B) mannans suspended in chloroform solution containing dissolved PHA.

Using the second method (only chloroform), different polymeric ratios (presented as PHB/mannans ratios) were tested, namely 25/75 % (w/w), 50/50 % (w/w) and 75/25 % (w/w). Both 25/75 % (w/w) and 50/50 % (w/w) ratios were discarded (figure 3.7 A and B, respectively), due to the incapacity to remove the films as a whole, caused by the rigid nature of the mannans layer. Using a 75/25 % (w/w) ratio (figure 3.7 C), the mannans layer was thinner and more flexible, and the amount of PHA located in the base layer was thick enough to endure the brittleness of the top layer (figure 3.7).

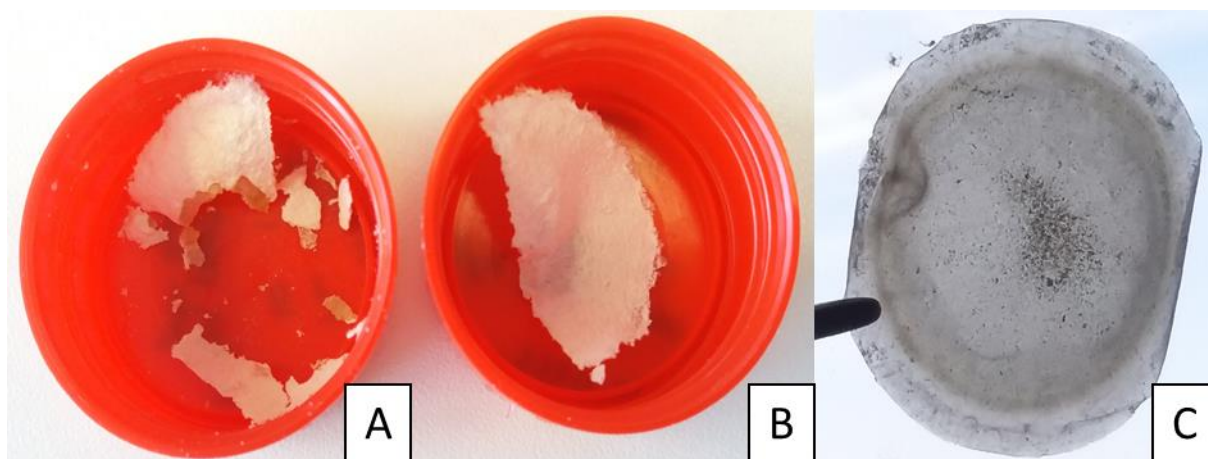


Figure 3.7. Different polymeric ratios for film formation.

(A) 25 % PHB, 75 % mannans; (B) 50 % PHB, 50 % mannans; (C) 75 % PHB, 25 % mannans.

Different PHAs were then used for film formation, either alone (100 % PHA) or in conjunction with mannans following the 75/25 % (w/w) ratio tested above. In total, 12 different PHA films were obtained, six pure and six mixture, namely 100PHB (100 % PHB), 75PHB (75/25 % (w/w) PHB/mannans), 100PHBHV17 (100 % PHBHV17), 75PHBHV17 (75/25 % (w/w) PHBHV17/mannans), 100PHBHV18 (100 % PHBHV18), 75PHBHV18 (75/25 % (w/w) PHBHV18/mannans), 100PHBHV27 (100 % PHBHV27), 75PHBHV27 (75/25 % (w/w) PHBHV27/mannans), 100PHBHV38 (100 % PHBHV38), 75PHBHV38 (75/25 % (w/w) PHBHV38/mannans), 100PHBHV56 (100 % PHBHV56) and 75PHBHV56 (75/25 % (w/w) PHBHV56/mannans), as shown in table 3.8. Pure PHA films (except 100PHBHV56) and 75PHB are presented in figure 3.8.

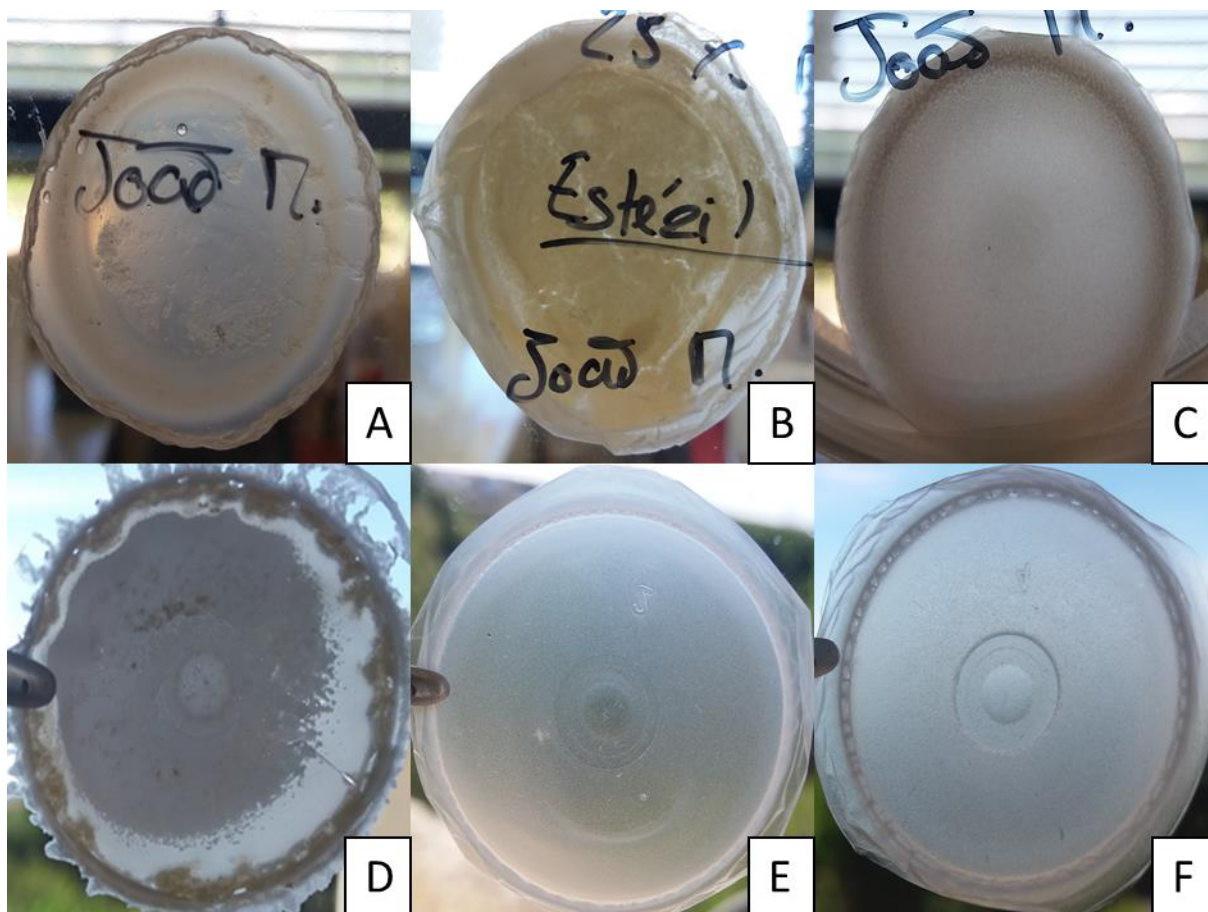


Figure 3.8. Some PHA films prepared for biological assays.

(A) 100PHB; (B) 75PHB; (C) 100PHBHV17; (D) 100PHBHV18; (E) 100PHBHV27; (F) 100PHBHV38.

Table 3.8. PHA films prepared for biological assays.

Film	PHA Used	PHA % (w/w)	Mannans % (w/w)	Malleability	Translucency
100PHB	PHB	100	0	+	+
75PHB	PHB	75	25	+	-
100PHBHV17	PHBHV17	100	0	+	+
75PHBHV17	PHBHV17	75	25	+	-
100PHBHV18	PHBHV18	100	0	-	-
75PHBHV18	PHBHV18	75	25	-	-
100PHBHV27	PHBHV27	100	0	++	+
75PHBHV27	PHBHV27	75	25	+	-
100PHBHV38	PHBHV38	100	0	++	+
75PHBHV38	PHBHV38	75	25	+	-
100PHBHV56	PHBHV56	100	0	++	+
75PHBHV56	PHBHV56	75	25	+	-

Results are presented as (-, absence; +, presence; ++, high presence).

All plain PHA films prepared were perfectly uniform and presented considerable malleability and translucency (with the exception of 100PHBHV18, which presented some rigidity and opacity, presumably due to the extraction process in which bleach was used) (figures 3.8 A, C, D, E and F). PHAs extracted with hypochlorite have been reported to have significant drawbacks in terms of weight and polydispersity when compared to PHAs extracted with chloroform, as hypochlorite interacts with the polymer, degrading it. The resulting polymer has a lower molecular weight (reported as 50 to 70 % loss of molecular weight), but also a higher polydispersity [24, 25]. Moreover, bleach has been

previously used to whiten PHAs [53], which could account for its increased opaqueness. The HV content also proved impactful on film malleability (ductility), as films with higher HV contents were considerably more malleable, as expected [54]. Regarding mixture films, the bottom PHA layer presented similar malleability to their pure counterparts for lower HV content films. Higher HV content films were less malleable than their pure counterparts, but similar to lower HV content films, most likely due to the top mannans layer. Translucency, however, was absent from mixture films due to the uniformly distributed top layer of mannans over the PHA layer (figure 3.8 B). All PHA films prepared were sterilized in autoclave (121 °C, 30 min), transferred to sealed petri dishes and laid aside for biological assays.

3.6. Cytotoxicity Assays

Cytotoxicity assays were performed for both original mannans and its deproteinized version, using HCT116, A2780 and normal fibroblasts. Results are displayed in figure 3.9.

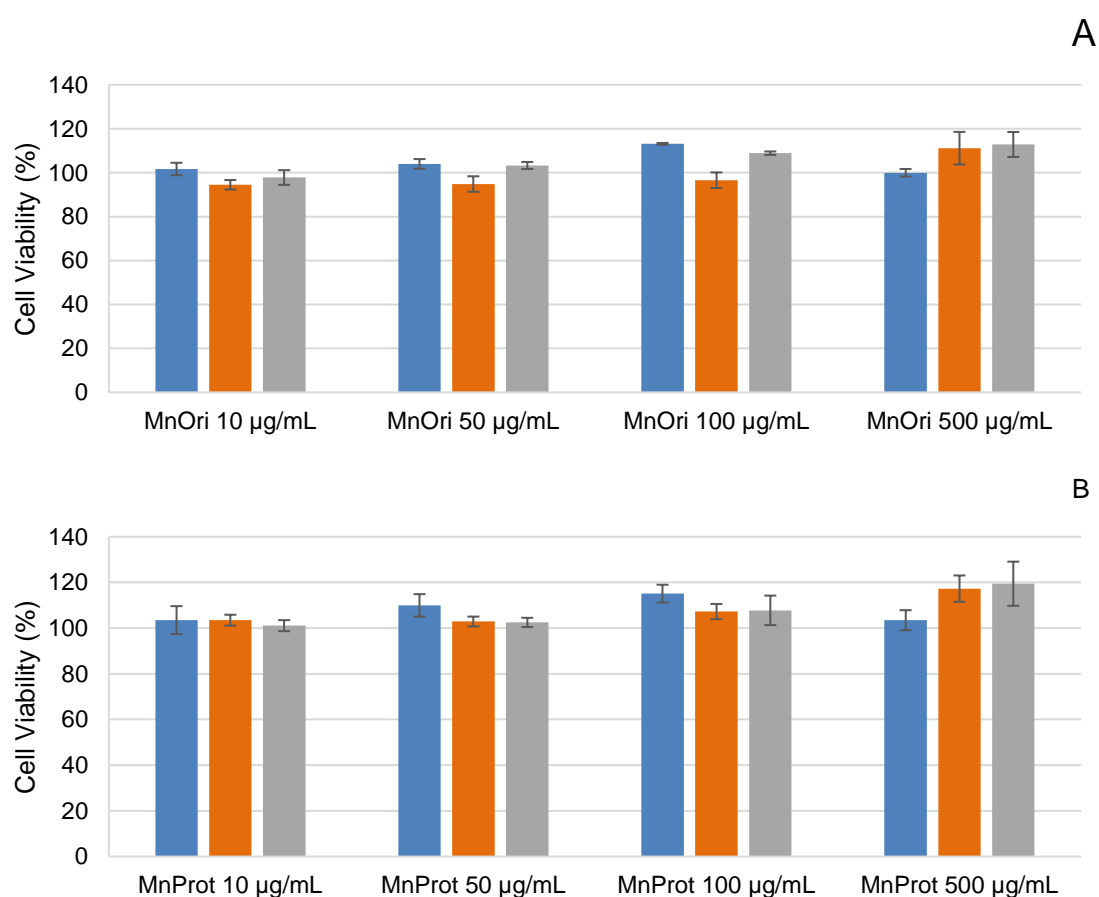


Figure 3.9. Mannans influence in cell viability.

(A) Effect of original mannans (MnOri); (B) Effect of deproteinized mannans (MnProt). Blue bars represent cell line A2780, orange bars represent cell line HCT116, grey bars represent normal skin fibroblasts cell line. Error bars represent the standard error of the mean of three independent assays.

Both mannans versions were tested, using the three cell lines mentioned, up to a maximum concentration of 500 $\mu\text{g mL}^{-1}$. For all concentrations of both polymers studied, no effect on cell viability was observed (cell viability remains near 100 %). This effect is observed for all cell lines tested (Figure 3.9). Furthermore, both polymers present very similar patterns, which most likely means that the proteins present in the original polymer have no influence on cell viability (Figure 3.9). Given this result, mannans were proven to have no cytotoxic effect on any of the cell lines tested, rendering them suitable to be used in further biological studies. Deproteinized mannans were discarded from further tests, as the proteins present in the original polymer also have no cytotoxic effect.

The original version of the polymer was also tested in skin fibroblasts, up to a concentration of 2000 $\mu\text{g mL}^{-1}$, aiming at a possible application of this polymer in wound dressing. Results are displayed in figure 3.10.

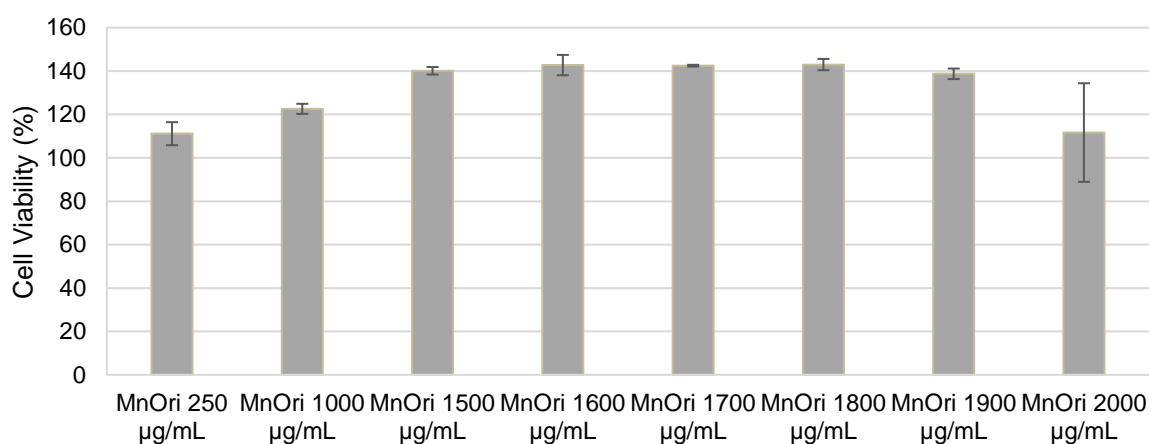


Figure 3.10. Mannans influence in normal skin fibroblast cell viability (high concentrations).

Grey bars represent normal skin fibroblasts cell line. Error bars represent the standard error of the mean of three independent assays.

In this assay, cell viability seems to slightly increase with the concentration of polymer in the medium (up to 1500 $\mu\text{g mL}^{-1}$) to as much as 140 % of its control value, opening the possibility that skin fibroblasts could use the polymer as a substrate, potentially raising the mitochondrial activity level (Figure 3.10). This effect is true up to 1900 $\mu\text{g mL}^{-1}$, from which it starts to diminish, presumably due to a high concentration of polymer which may impair good homogenizing of the medium, preventing cell access to certain nutrients. Nevertheless, cell viability remains near 100 % (Figure 3.10).

Wound regeneration is a complex process, coordinating the activity of different cell lines as well as growth factors and matrix signals. Among the major players in this process are dermal fibroblasts, which migrate to the site of the skin lesion, and are responsible for the production of a collagen-rich matrix which supports epidermal cells and allows them to proliferate and reform the skin [55]. Mannans are hereby proven to increase skin fibroblast cell viability, which can be translated in one of two occurrences: an increase in the mitochondrial activity of the cell, or an increase in the total number

of cells. Further tests, such as dsDNA quantification or protein quantification, could be performed to determine which of these is true [56].

At any rate, if skin fibroblasts are able to use the polymer as a substrate, by means of its degradation (degrading mannans to their respective monomers, mainly mannose), this polymer could end up being used in wound healing in more than just a fibroblast stimulant. Scarring is also an important factor in wound healing, which is highly mediated by TGF- β 1 (one of the growth factors which induce fibroblasts to produce the collagen-rich matrix). In adults, TGF- β 1 remains at the wound site for prolonged periods of time, even after the collagen matrix is completed, contributing to the formation of scarred tissue. Although specific antibodies or TGF- β 3 have been used before to inhibit TGF- β 1, mannose-6-phosphate (M-6-P) has also been described to inhibit TGF- β 1, by means of the (M-6-P)-IGF II receptor [55]. As such, mannans degraded into mannose by the fibroblasts could prove valuable in preventing scarring, more so if the polymer has a high degree of phosphorylation.

3.7. Cell Adherence Assays

3.7.1. Polysaccharide Films

Cell adherence assays were conducted in skin fibroblasts using the mannans films (MnOri30, MnOri-90, MnOriFeFilm, MnOriFeNaOHFilm, MnOriFeBeads30 and MnOriFeBeads-90) in an attempt to test their capability to be used as an adherence matrix for wound dressing applications (figure 3.11).

Immediately after the addition of the cell suspension, MnOri-90 (figure 3.11 B) and MnOriFeBeads-90 (figure 3.11 D) films obtained by freeze drying disintegrated and solubilized, rendering this drying method impractical for this application. This effect was most likely caused by the large contact surface area between the polymer and the cell culture medium, causing the matrix to collapse and dissolve. MnOri30 completely disintegrated and solubilized after the 24 h period given for cell adhesion in biological assays (figure 3.11 A). Mannans are highly soluble in water and, despite the tight structure of the film, the polymer quickly solubilized especially when submitted to a higher temperature (37 °C) than room temperature.

With respect to MnOriFeBeads30 (figure 3.11 C) and MnOriFeFilm (figure 3.11 E) films, a complete loss of all their structure was observed after the 24 h incubation period, however they did not completely solubilize. Particles of their original structure were still visible attached to the bottom of the cell culture plate, but the most part was suspended in the culture medium. This leads to the conclusion that the mixture of polymer and iron salt was highly imperfect, as the most part of the two films was still soluble, presenting just a few insoluble particles. Regarding MnOriFeFilm (figure 3.11 E), only a coat of iron could be achieved on top of the original film prepared, which could have been disrupted and separated from the inside uncoated part, probably due the temperature used. Another possible explanation could be the lack of NaOH in the film formation process, making the iron coat simply less soluble, yet not insoluble. MnOriFeBeads30 (figure 3.11 C) were prepared using a mixture of the polymer and the iron salt dissolved in deionized water, which does not support the hypothesis of the

poor mixture of the two components. The fact that the corresponding beads are only formed after they are dropped in the NaOH solution could present an explanation, as only the outer layer becomes truly insoluble by the action of the alkaline solution, and the integrity of the shell of the beads could be compromised by the drying process, thus rendering them useless by exposing part of their interior soluble fraction. This later explanation, however, does not support what happened with the last film, MnOriFeNaOHFilm (figure 3.11 F). This film suffered an identical transformation process to the beads (iron salt followed by NaOH) thus forming the iron coat made insoluble by the action of the alkaline solution but did not disintegrate after the 24 h period of cell incubation as the previous two experiments, which leads to the conclusion that the coat was not compromised by the drying process and thus did not expose any interior soluble components. As to the difference between the beads film (MnOriFeBeads30) and the MnOriFeNaOHFilm film, the latter has a tighter interior, making it more resistant to fractures during the drying process which could account for the different results.

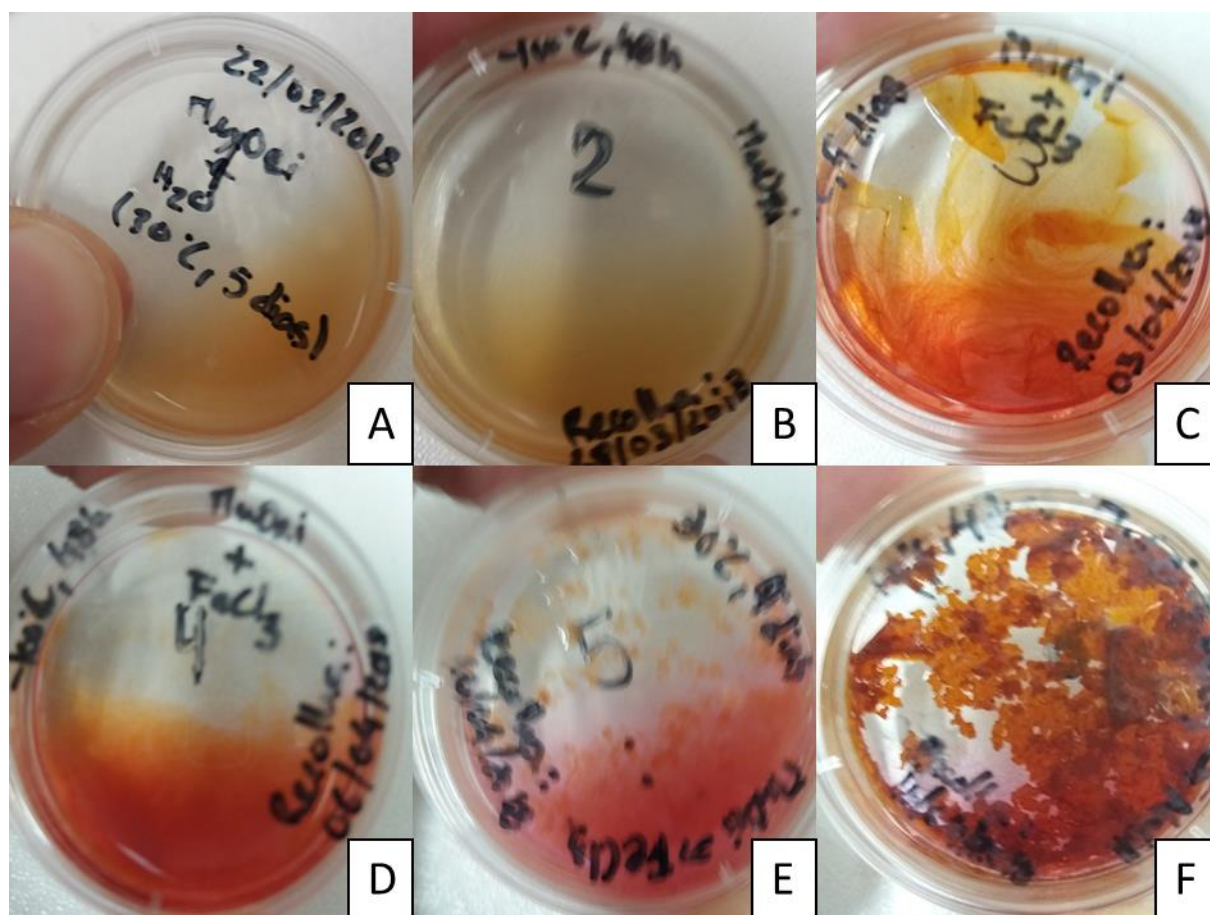


Figure 3.11. Mannans films used in cell adherence assays.

(A) MnOri30 after the 24 h incubation period; (B) MnOri-90 immediately after adding the cell suspension; (C) MnOriFeBeads30 after the 24 h incubation period; (D) MnOriFeBeads-90 immediately after adding the cell suspension; (E) MnOriFeFilm after the 24 h incubation period; (F) MnOriFeNaOHFilm after the 24 h incubation period. All cell culture plates are tilted for better visualization of either dissolution or suspension of the films in the culture medium.

Still, after microscopic observation of MnOriFeNaOHFilm after the cell adherence period (figure 3.12), no cells were visible on top of the film, and as such this line of research was abandoned.

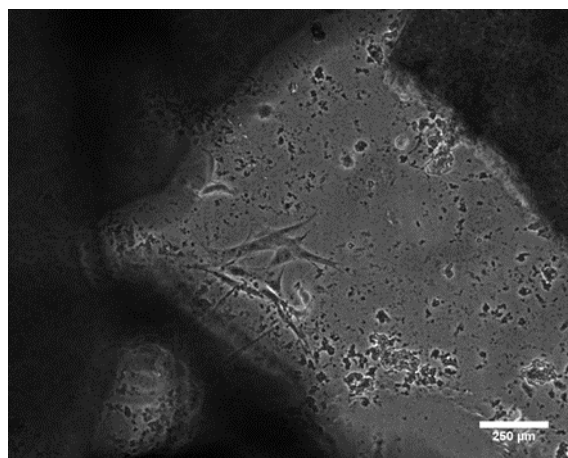


Figure 3.12. Microscopic observation of MnOriFeNaOHFilm after the cell adherence period (24 h).

The film corresponds to the darker section, whereas the lighter section corresponds to the bottom of the cell culture plate. Normal skin fibroblasts are visible adherent to the cell culture plate, displaying an elongated structure. No visible cells are found in the film section. The figure was obtained with total ampliation of 40x (10x ocular and 4x objective), and the scale bar represents 250 μm.

3.7.2. Polyester Films

All twelve PHA films were used in cell adherence studies. PHB, PHBHV17 and 100PHBHV18 were tested using skin fibroblasts and MCF7-GFP, and the other PHA films were tested only in MCF7-GFP (MCF7 cells modified to produce GFP, a green fluorescent protein). Skin fibroblasts were initially used as a target for these polymers' application, namely in wound dressing. However, microscopic observation of adherent cells was not always possible due to the film opacity, and so MCF7-GFP were used instead, using fluorescence as differentiation from the film structure. The use of fluorescent protein modified cells was also subject of difficult observation, as PHA polymers were discovered to have fluorescence of their own, although not as much as modified MCF7 cells. Microscopical observation of adherent cells is presented from figure 3.13 to figure 3.24.

Overall, PHA films proved capable of supporting cell adherence. In pure PHA films (100 % PHA) it was possible to observe multiple cells, both when using fibroblasts (observed in brightfield) or MCF7-GFP (observed using fluorescence filters) (figures 3.13, 3.15, 3.19, 3.21 and 3.23). Cells were able to adhere to 100PHB (figure 3.13 A, C, D and E), 100PHBHV17 (figure 3.15 A, C, D and E), 100PHBHV27 (figure 3.19 B, C and D), 100PHBHV38 (figure 3.21 B, C and D) and 100PHBHV56 (figure 3.23 B, C and D). However, when considering 100PHBHV18 films (figure 3.17 A, C, D and E), an inefficient adherence was observed, as no cells were visible on its surface. This might be due to i) the nature of its extraction (using bleach as a membrane disrupting agent) rendering the film opaquer and thus hindering visualization, or ii) an incomplete purification of the same, in which remnants of bleach could act against the cells.

Regarding the mannans/PHA films blends, visualization of adherent cells was hindered by the upper

layer of mannans, which were opaquer than the lower layer of PHA. Nevertheless, cells could still be observed using fluorescence filters, though in a much lower extent, in 75PHB (figure 3.14 A, C, D and E) and 75PHBHV38 mixture films (figure 3.22 B, C and D). While the diminishing of visually adherent cells was to be expected by the opacity factor in play, there was no visual observation of adherent cells in either of the other blend films (figures 3.16, 3.18, 3.20 and 3.24).

Films made of homopolymer PHB and co-polymeric PHB blends, such as P(3-HB-co-4-HB), have been investigated for their in vitro capacity to support cell adherence, and proved suitable to be used as porous matrices for applications such as wound dressing. It was discovered that films made of these polymers were good matrices for cell growth, with multiple sized pores interconnected in the film structure suitable for nutrients diffusion and cellular waste disposal. Moreover, cell adhesion assays displayed several fibroblasts attached to the PHB matrix surface, which are in agreement with the results obtained in this work [40, 41].

In the cited literature, however, these results pale in comparison to those obtained for blended PHAs, namely PHB or P(3-HB-co-4-HB) with polysaccharides. Using bacterial cellulose to produce polymeric blends with the aforementioned polyesters, Zhijiang and co-workers discovered that the new polyester-polysaccharide blends were even more suitable for biological applications [40, 41]. Films made from these new blends had a better internal pore structure, as well as a polysaccharide matrix to aid protein anchoring to the film, allowing cells to adhere with more ease. More fibroblast cells were found adherent to these structures, as well as a change in their morphology which suggested they were proliferating. As such, these blend matrices were found to be much better suited for biological applications such as wound dressing [40, 41]. These results are hard to compare with the ones obtained in this work. The blend films in the cited literature were prepared in a different way (using a solvent adequate for dissolving both polymers, TFA) and therefore there was no double layer with polymer segregation, and also another polysaccharide was used, which has a different composition. These matrices were more homogenous and resulted in a better cell adherence, which was not observed in this study. Despite that fact, cells were found to adhere to some of the blended polymeric matrices in this study. Considering the mentioned difficulty in the observation of adherent cells and the results published for other polyester-polysaccharide blends, it is reasonable to assume that, if better polyester-polysaccharide blends are achieved, their resulting films could provide a better adherence surface, and therefore used in tissue regeneration applications.

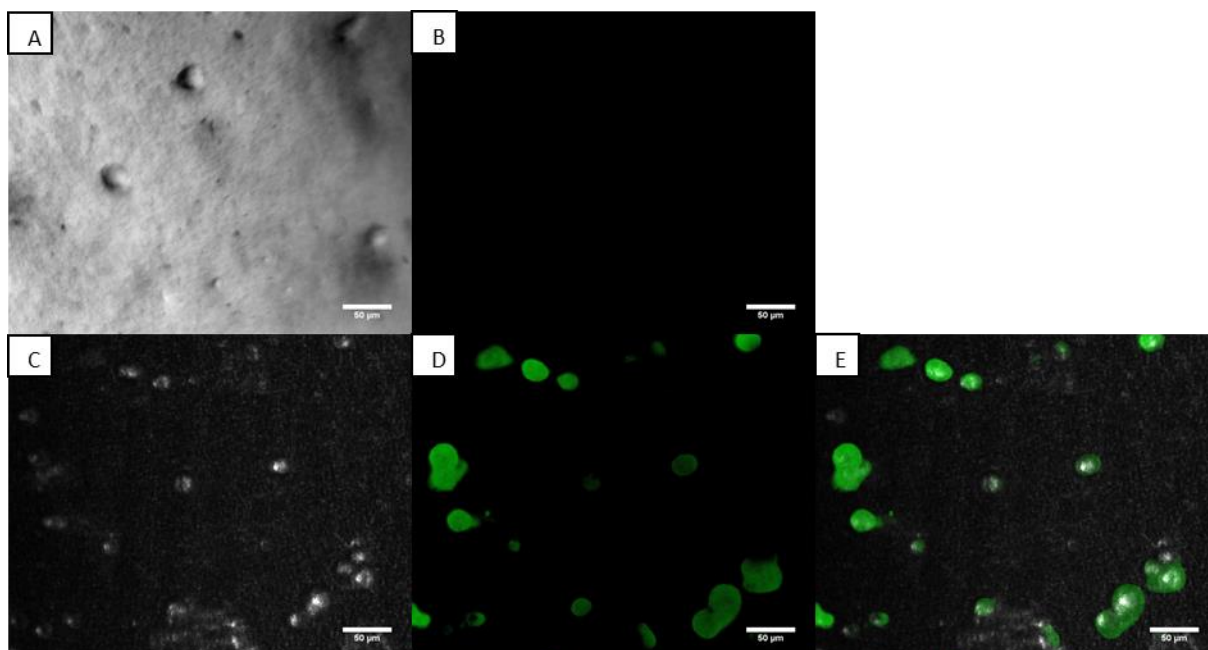


Figure 3.13. Cell growth in 100PHB films.

(A) 100PHB with skin fibroblasts (Brightfield); (B) 100PHB with no cells (Blue excitation); (C) 100PHB with MCF7-GFP (Brightfield); (D) 100PHB with MCF7-GFP (Blue excitation); (E) Superimposed images of 100PHB with MCF7-GFP in brightfield and blue excitation (figures C and D). In figures (A) and (C) cells are round projections on the film surface, and in figures (D) and (E) cells are green spots on the film surface. All figures were obtained with total amplification of 200x (10x ocular and 20x objective), and the scale bar represents 50 μm .

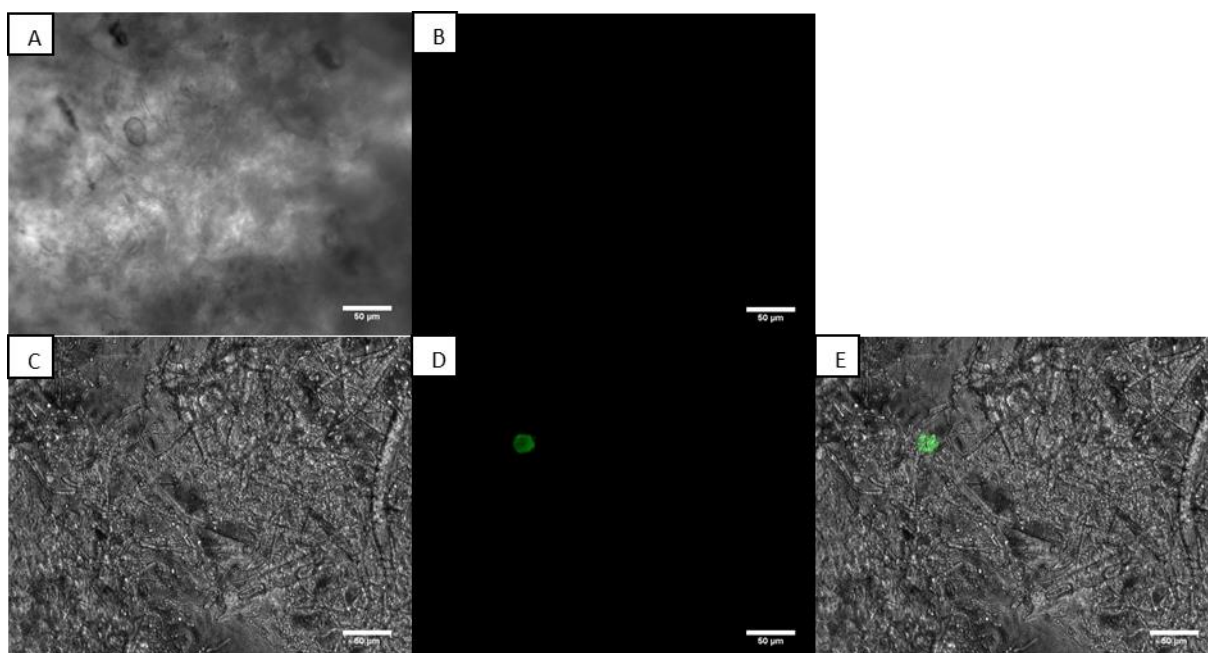


Figure 3.14. Cell growth in 75PHB films.

(A) 75PHB with skin fibroblasts (Brightfield); (B) 75PHB with no cells (Blue excitation); (C) 75PHB with MCF7-GFP (Brightfield); (D) 75PHB with MCF7-GFP (Blue excitation); (E) Superimposed images of 75PHB with MCF7-GFP in brightfield and blue excitation (figures C and D). In figures (A) and (C) cells are round projections on the film surface, and in figures (D) and (E) cells are green spots on the film surface. All figures were obtained with total amplification of 200x (10x ocular and 20x objective), and the scale bar represents 50 μm .

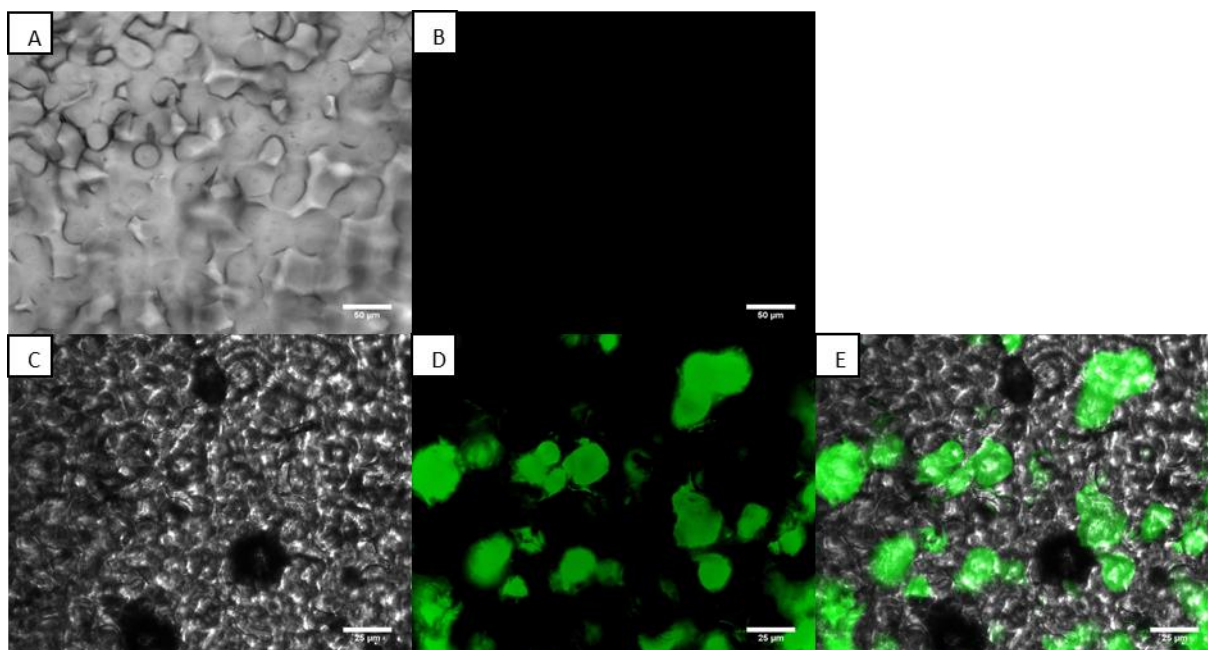


Figure 3.15. Cell growth in 100PHBHV17 films.

(A) 100PHBHV17 with skin fibroblasts (Brightfield); (B) 100PHBHV17 with no cells (Blue excitation); (C) 100PHBHV17 with MCF7-GFP (Brightfield); (D) 100PHBHV17 with MCF7-GFP (Blue excitation); (E) Superimposed images of 100PHBHV17 with MCF7-GFP in brightfield and blue excitation (figures C and D). In figures (A) and (C) cells are round projections on the film surface, and in figures (D) and (E) cells are green spots on the film surface. Figures (A) and (B) were obtained with total amplification of 200x (10x ocular and 20x objective), and the scale bar represents 50 μm . Figures (C), (D) and (E) were obtained with total amplification of 400x (10x ocular and 40x objective), and the scale bar represents 25 μm .

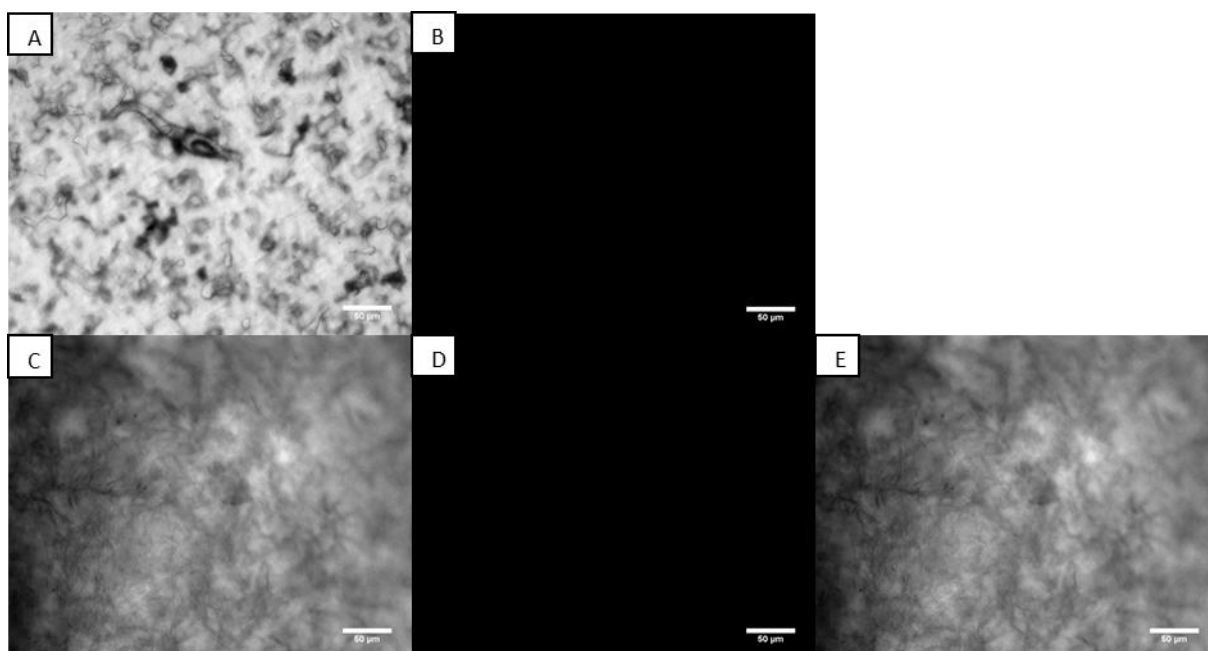


Figure 3.16. Cell growth in 75PHBHV17 films.

(A) 75PHBHV17 with skin fibroblasts (Brightfield); (B) 75PHBHV17 with no cells (Blue excitation); (C) 75PHBHV17 with MCF7-GFP (Brightfield); (D) 75PHBHV17 with MCF7-GFP (Blue excitation); (E) Superimposed images of 75PHBHV17 with MCF7-GFP in brightfield and blue excitation (figures C and D). In figures (A) and (C) cells are round projections on the film surface, and in figures (D) and (E) cells are green spots on the film surface. All figures were obtained with total amplification of 200x (10x ocular and 20x objective), and the scale bar represents 50 μm .

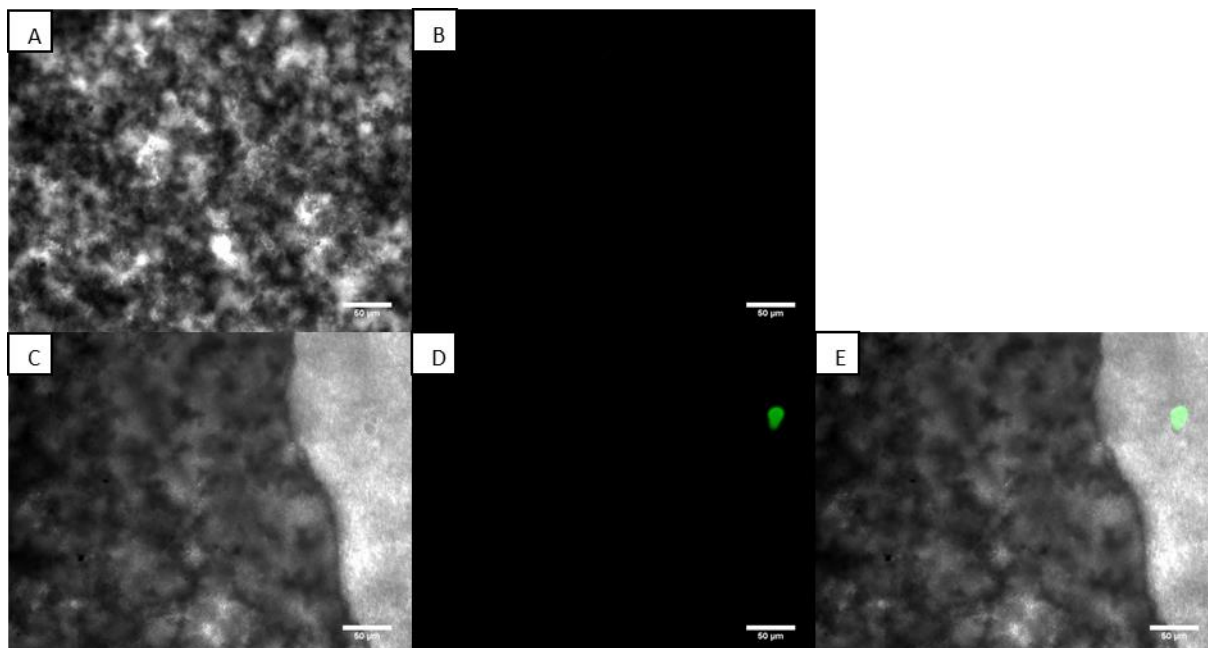


Figure 3.17. Cell growth in 100PHBHV18 films.

(A) 100PHBHV18 with skin fibroblasts (Brightfield); (B) 100PHBHV18 with no cells (Blue excitation); (C) 100PHBHV18 with MCF7-GFP (Brightfield); (D) 100PHBHV18 with MCF7-GFP (Blue excitation); (E) Superimposed images of 100PHBHV18 with MCF7-GFP in brightfield and blue excitation (figures C and D). In figures (A) and (C) cells are round projections on the film surface, and in figures (D) and (E) cells are green spots on the film surface. All figures were obtained with total amplification of 200x (10x ocular and 20x objective), and the scale bar represents 50 μm .

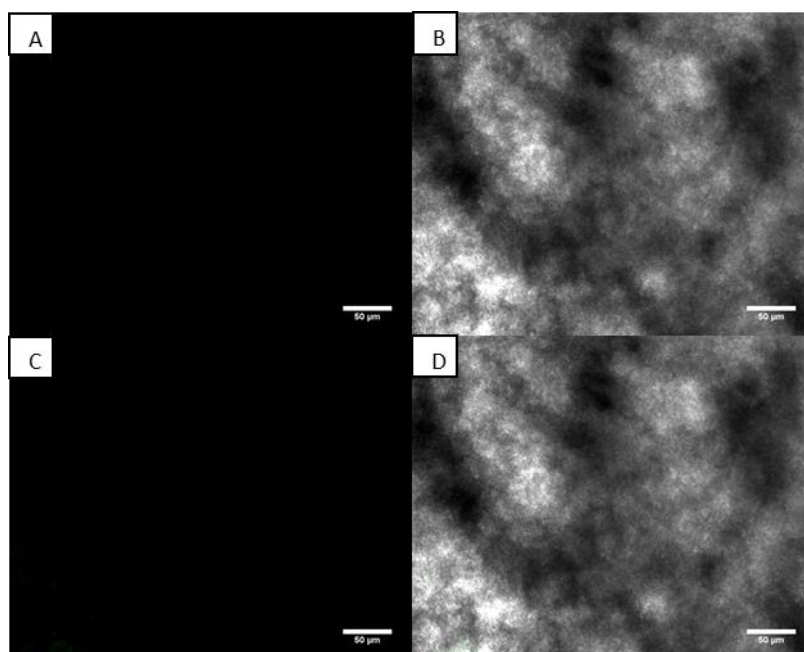


Figure 3.18. Cell growth in 75PHBHV18 films.

(A) 75PHBHV18 with no cells (Blue excitation); (B) 75PHBHV18 with MCF7-GFP (Brightfield); (C) 75PHBHV18 with MCF7-GFP (Blue excitation); (D) Superimposed images of 75PHBHV18 with MCF7-GFP in brightfield and blue excitation (figures B and C). In figure (B) cells are round projections on the film surface, and in figures (C) and (D) cells are green spots on the film surface. All figures were obtained with total amplification of 200x (10x ocular and 20x objective), and the scale bar represents 50 μm .

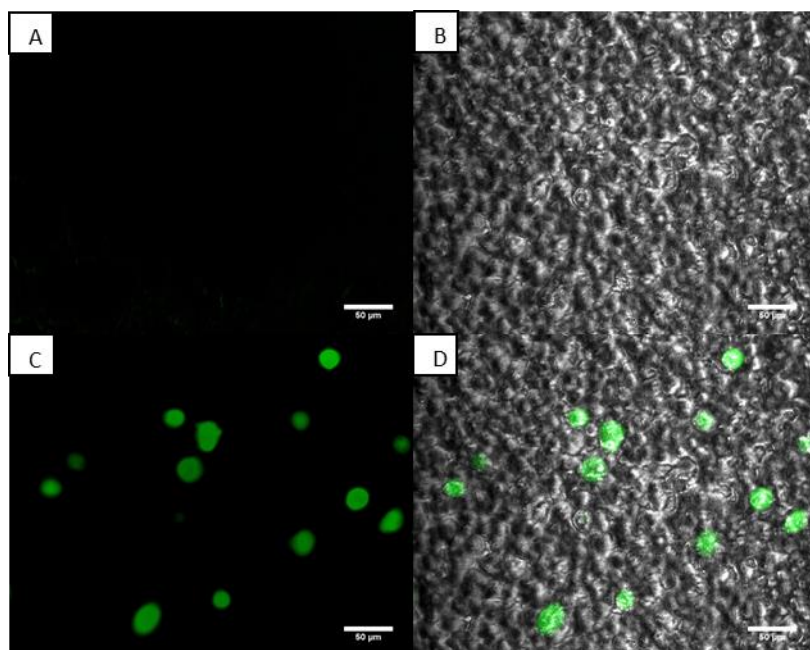


Figure 3.19. Cell growth in 100PHBHV27 films.

(A) 100PHBHV27 with no cells (Blue excitation); (B) 100PHBHV27 with MCF7-GFP (Brightfield); (C) 100PHBHV27 with MCF7-GFP (Blue excitation); (D) Superimposed images of 100PHBHV27 with MCF7-GFP in brightfield and blue excitation (figures B and C). In figure (B) cells are round projections on the film surface and in figures (C) and (D) cells are green spots on the film surface. All figures were obtained with total amplification of 200x (10x ocular and 20x objective), and the scale bar represents 50 µm.

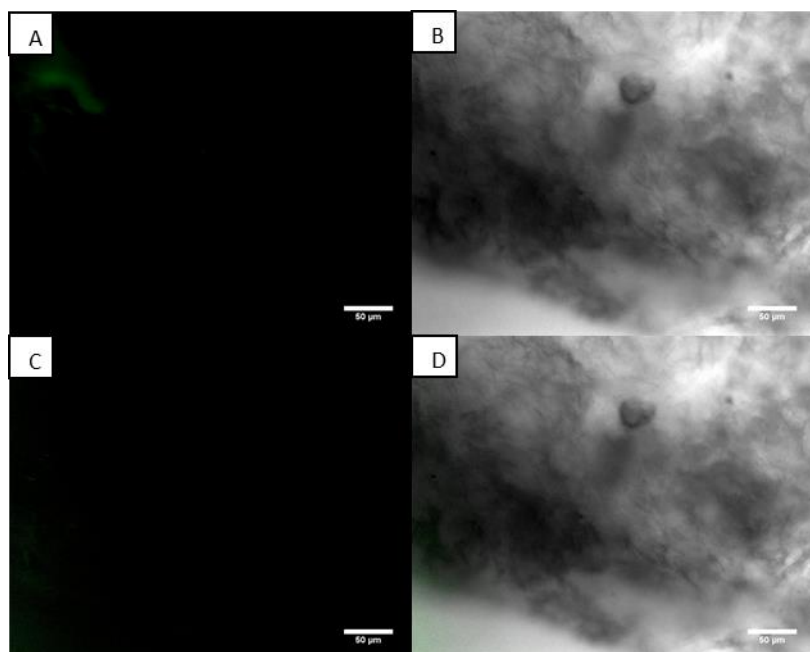


Figure 3.20. Cell growth in 75PHBHV27 films.

(A) 75PHBHV27 with no cells (Blue excitation); (B) 75PHBHV27 with MCF7-GFP (Brightfield); (C) 75PHBHV27 with MCF7-GFP (Blue excitation); (D) Superimposed images of 75PHBHV27 with MCF7-GFP in brightfield and blue excitation (figures B and C). In figure (B) cells are round projections on the film surface and in figures (C) and (D) cells are green spots on the film surface. All figures were obtained with total amplification of 200x (10x ocular and 20x objective), and the scale bar represents 50 µm.

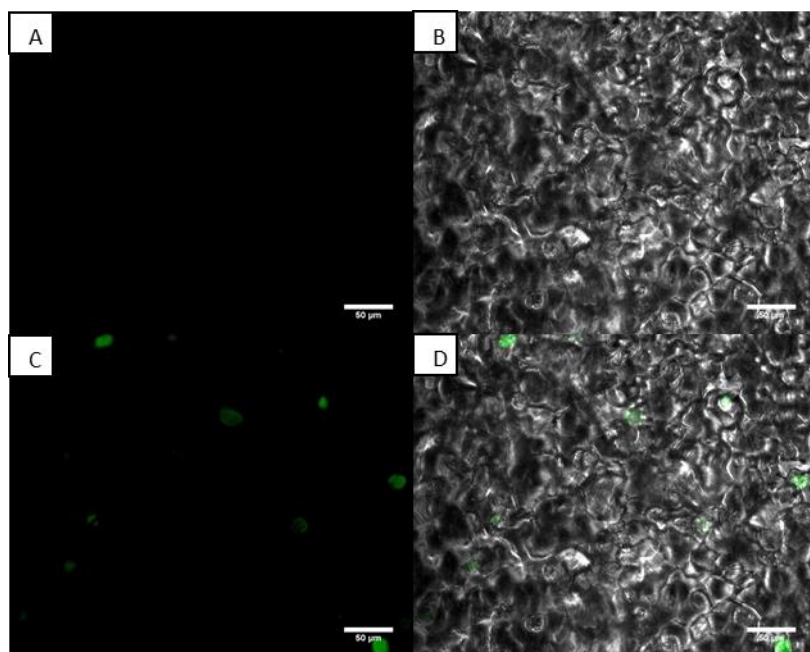


Figure 3.21. Cell growth in 100PHBHV38 films.

(A) 100PHBHV38 with no cells (Blue excitation); (B) 100PHBHV38 with MCF7-GFP (Brightfield); (C) 100PHBHV38 with MCF7-GFP (Blue excitation); (D) Superimposed images of 100PHBHV38 with MCF7-GFP in brightfield and blue excitation (figures B and C). In figure (B) cells are round projections on the film surface and in figures (C) and (D) cells are green spots on the film surface. All figures were obtained with total ampliation of 200x (10x ocular and 20x objective), and the scale bar represents 50 μm .

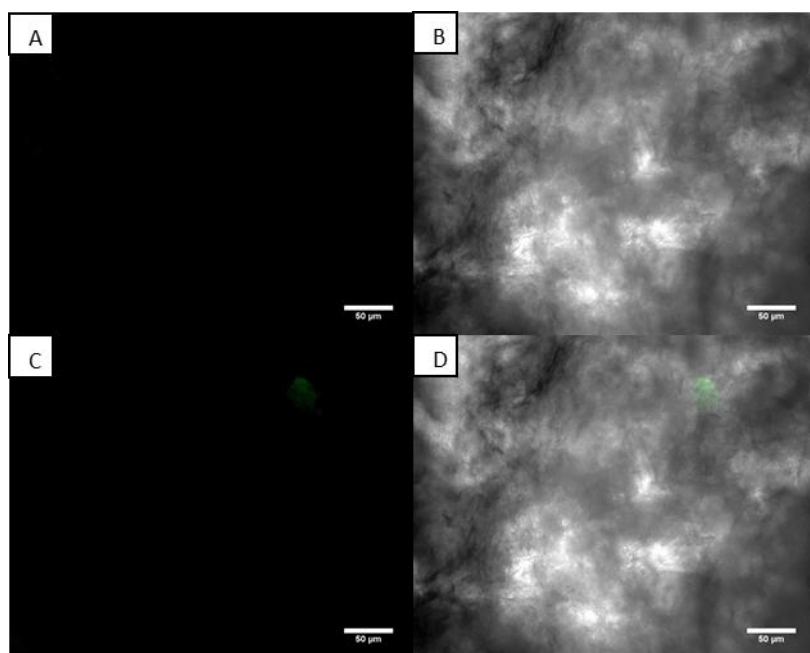


Figure 3.22. Cell growth in 75PHBHV38 films.

(A) 75PHBHV38 with no cells (Blue excitation); (B) 75PHBHV38 with MCF7-GFP (Brightfield); (C) 75PHBHV38 with MCF7-GFP (Blue excitation); (D) Superimposed images of 75PHBHV38 with MCF7-GFP in brightfield and blue excitation (figures B and C). In figure (B) cells are round projections on the film surface and in figures (C) and (D) cells are green spots on the film surface. All figures were obtained with total ampliation of 200x (10x ocular and 20x objective), and the scale bar represents 50 μm .

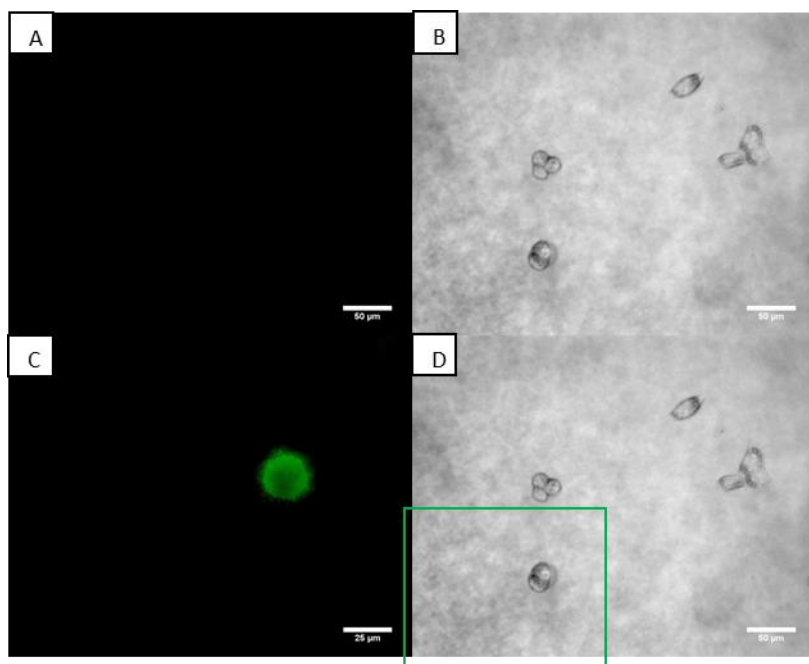


Figure 3.23. Cell growth in 100PHBHV56 films.

(A) 100PHBHV56 with no cells (Blue excitation); (B) 100PHBHV56 with MCF7-GFP (Brightfield); (C) 100PHBHV56 with MCF7-GFP (Blue excitation); (D) 100PHBHV56 with MCF7-GFP (Brightfield), with a green rectangle delimiting to the area where figure (C) would superimpose. In figures (B) and (D) cells are round projections on the film surface and in figure (C) cells are green spots on the film surface. Figures (A), (B) and (D) were obtained with total amplification of 200x (10x ocular and 20x objective), and the scale bar represents 50 μm . Figure (C) was obtained with total amplification of 400x (10x ocular and 40x objective), and the scale bar represents 25 μm .

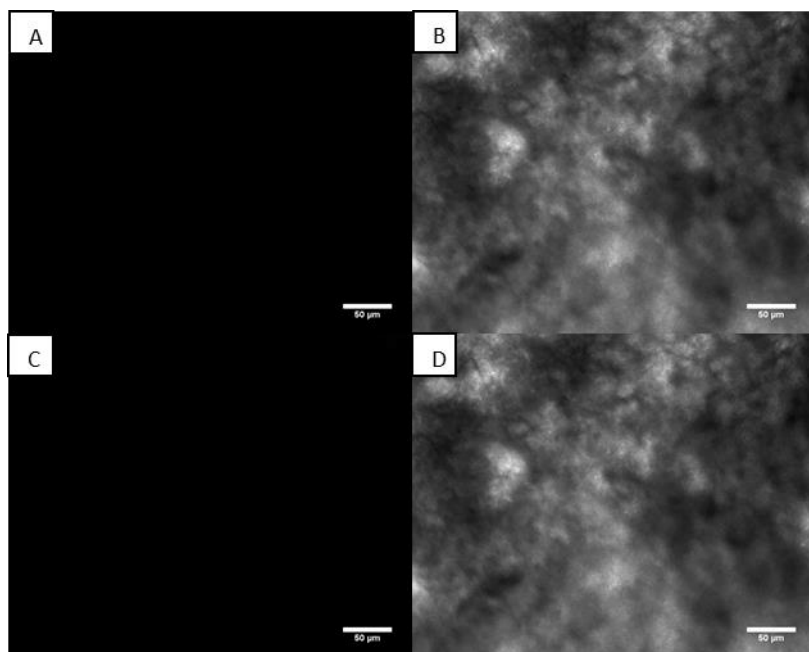


Figure 3.24. Cell growth in 75PHBHV56 films.

(A) 75PHBHV56 with no cells (Blue excitation); (B) 75PHBHV56 with MCF7-GFP (Brightfield); (C) 75PHBHV56 with MCF7-GFP (Blue excitation); (D) Superimposed images of 75PHBHV56 with MCF7-GFP in brightfield and blue excitation (figures B and C). In figure (B) cells are round projections on the film surface and in figures (C) and (D) cells are green spots on the film surface. All figures were obtained with total amplification of 200x (10x ocular and 20x objective), and the scale bar represents 50 μm .

Cell viability was also tested for adherent cells on some PHA films (using MCF7-GFP), based on the previous results for cell adherence and polymer availability. Regarding the results for cell adherence, only 100 % PHA films were selected. Also, of the six different polymers previously tested, PHB and PHBHV56 were unavailable. As such, only four different films were selected, namely 100PHBHV17, 100PHBHV18, 100PHBHV27 and 100PHBHV38 (figure 3.25).

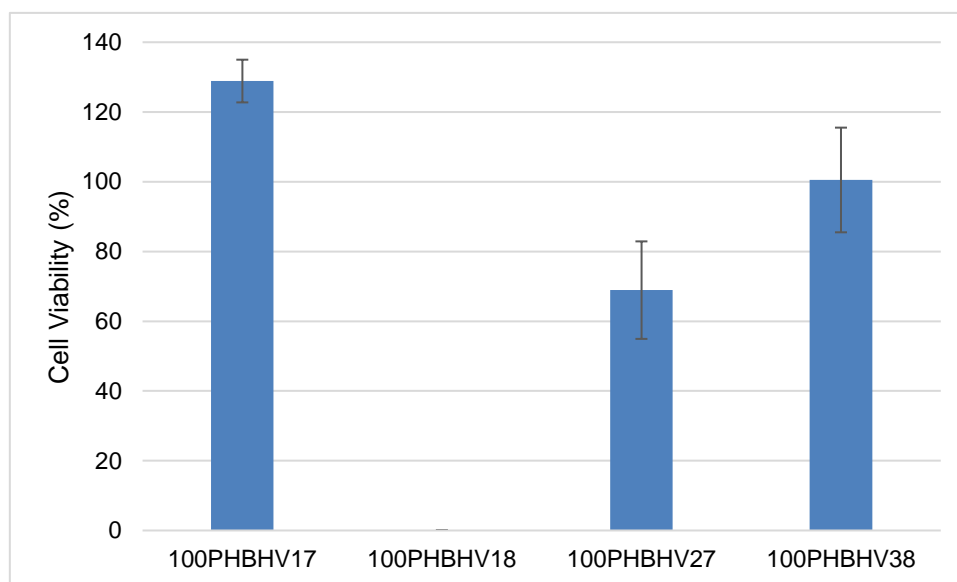


Figure 3.25. Cell viability of adherent MCF7-GFP cells in different PHA films.

Blue bars represent cell line MCF7-GFP. Error bars represent the standard error of the mean of two independent assays.

When observing figure 3.25, no correlation between film composition and cell viability was observed. 100PHBHV17 and 100PHBHV38 films show no cytotoxicity (> 100 % cell viability), while 100PHBHV27 shows a slightly decrease of cell viability (figure 3.25). Regarding cells tested on 100PHBHV18 films, a complete loss of cell viability was observed (figure 3.25). This result is in agreement with the possibility that this polymer's purification might have been unsuccessful, leaving residual bleach in the polymer which could hinder cell growth. Reported studies performed using PHB and PHBHV films *in vitro* are sometimes contradictory, due to the experimental conditions that greatly affect the results. It has been reported that an increase in HV content may be responsible for a slight decrease in cell viability *in vitro*. However, different studies appointed causes for this phenomena related to the purity of the polymers used (in terms of cell debris, such as saturated fatty acids) rather than the HV content, and reported that highly purified polyesters with varying HV contents are equally biocompatible [39], which could explain the differences observed in figure 3.25, meaning that 100PHBHV27 could have simply been prepared from a less purified polymer.

Overall, the matrices prepared from PHAs extracted and purified with chloroform were biocompatible and proved capable of supporting cell adherence *in vitro*, especially when made solely of polyester. The hypochlorite extraction method proved inefficient in yielding PHAs for biological applications, as a

similar purification method employed for the chloroform extracted PHAs was used, which in this case was apparently not effective. Also, as previously discussed, a different method for obtaining polyester-polysaccharide blends could yield better results for cell adherence, as described in the cited literature. Nevertheless, the results obtained are inconclusive in that regard derived from the observation constraints imposed by the opacity of the films.

Chapter 4. Conclusions and Future Work

In this thesis, two different polymers were used to prepare structures for biomedical applications, namely polysaccharide gel particles for drug delivery and polymeric films for both drug delivery and wound dressing applications.

Mannans were produced by *K. pastoris* using glycerol as carbon source and polyhydroxyalkanoates (PHAs) were produced by mixed cultures using fermented fruit pulp waste.

Two transformation procedures were tested in mannans, a deproteinization and a phosphorylation procedure. The deproteinization was partially successful, removing 69.49 ± 0.44 % of the total protein of the mannans sample, but reduced the available polymer to 41.19 ± 1.73 %. The phosphorylation procedure was unsuccessful. Only 29.72 % of the sample was able to be recovered, with a total loss in phosphate groups of 60.45 ± 1.23 %.

Mannans and their deproteinized version were tested in normal fibroblasts, A2780 and HCT116 cell lines, and were found to have no cytotoxicity for either of the cell lines tested, proving mannans could be used in future biological assays and rendering the deproteinization method an unnecessary step for mannans to be used in biological applications.

This polysaccharide was then used to prepare biopolymeric matrices for medical applications. Mannans were firstly investigated for their capability to form gels. Different methods were used, and the effect of temperature, pH and salt concentration was tested. Mannans were found to gel under low temperature (4 °C) and alkaline pH, and under preferential interaction with higher concentrations of iron and copper salts. Gel particles were developed considering the gelling conditions described above, using six different methods. The effect of cation valence was also tested. The method using a tri-valent cation (iron) followed by NaOH yielded the best gel particles regarding their stability.

Mannans were also used to prepare films, and the effect of plasticizers (glycerol and polyethylene glycol) was tested. In the concentrations used, the plasticizers had no positive effect, and were consequently discarded. Mannans films were also tested for their drying process, and films dried at 30 °C or freeze dried were obtained. Mannans films were also used to develop a new type of insoluble film following the gelation procedures tested with iron salts, and two methods were accomplished, using a previously prepared film dipped in an iron salt solution, and then either dipped in a NaOH solution or not. Also, gel beads obtained in method 4 for gelation procedures were used to prepare films. In total, six different films (mannans film dried at 30 °C, mannans film freeze dried, mannans film dipped in iron solution, mannans film dipped in iron solution and NaOH solution, mannans gel beads dried at 30 °C and mannans gel beads freeze dried) were tested in fibroblasts. Of those six, only the mannans film dipped in iron solution and NaOH solution resisted the cell growth conditions, but no cells were visible attached to it.

PHAs with different compositions (pure PHB and co-polymeric PHBHV with different HV contents)

were used to produce films, alone and blended with mannans. The process of blending PHA and mannans was investigated, regarding the solvent used and the proportions of both polymers. Chloroform was the elected solvent for the PHA-mannans blending process, and optimal PHA-mannans ratio for that blending process was achieved at 75 % PHA and 25 % mannans. Blended films had a two-layer structure with apparent segregation of polymers, composed of a PHA bottom layer and a mannans top layer.

Twelve different films (six pure PHA and six blends) were produced and tested in normal fibroblasts or MCF7-GFP cell line. Overall, pure PHA films were found adequate for cell adherence, with the exception of the film made of PHBHV with an HV content of 18 %, most likely due to the inefficient extraction process it was submitted to. Blended PHA-mannans films were found mostly incapable of supporting cell adhesion, with visible adherent cells in only two blend films (75PHB and 75PHBHV38) and to a much lower extent than their pure counterparts. This could be due to the blending process, since blended PHA-polysaccharide films were found adept for cell adhesion in the literature. Pure PHA films were also tested for their cytotoxicity. The results confirmed the observations made in the cell adherence assays, as most PHA films showed no cytotoxicity. The film made of PHBHV with 18 % HV was also shown to be cytotoxic for the cells, supporting the claims of a hypochlorite contamination due to an inefficient extraction process.

As for future work, much is left undone. First of all, as discussed, phosphomannans have been described as having antitumor activity. More than just a drug delivery system, this polymer could act as a cancer pharmaceutical by itself, and therefore different methods to yield such a polymer should be tested.

On a second note, in this thesis mannans gel particles have been successfully obtained, but the method could still be optimized, as their stability could be improved. These gel beads were not verified for their cytotoxic activity, metal release profiles, or encapsulation of pharmaceuticals, which is yet to be tested.

Lastly, most of the pure PHA films in use have shown great potential for cell adhesion assays and further studies should be carried out, including an extensive characterization of these matrices, as well as their capacity to incorporate pharmaceuticals for drug delivery. Their blend counterparts, however, left a lot to be desired. This was an unexpected result, as the supporting literature clearly states the potential of such films. In this regard, the method used for blending should be revisited. The most likely route would be a method involving a solvent which could dissolve both polymers, such as TFA, to achieve proper homogenization of the matrix.

Chapter 5. Bibliography

- [1] Aravamudhan A, Ramos DM, Nada AA, et al. Natural Polymers: Polysaccharides and Their Derivatives for Biomedical Applications. In: Natural and Synthetic Biomedical Polymers Elsevier Inc. 2014; pp. 67–89.
- [2] Bassas-Galia M, Follonier S, Pusnik M, et al. Natural polymers: A source of inspiration. In: Bioresorbable Polymers for Biomedical Applications: From Fundamentals to Translational Medicine Elsevier Ltd 2016; pp. 31–64.
- [3] Freitas F, Roca C, Reis MAM. Fungi as Sources of Polysaccharides for Pharmaceutical and Biomedical Applications. In: Handbook of Polymers for Pharmaceutical Technologies 2015; bk. 3, pp. 61–103.
- [4] Christian P. Polymer chemistry. In: Electrospinning for Tissue Regeneration 2011; pp. 34–50.
- [5] Nwodo UU, Green E, Okoh AI. Bacterial Exopolysaccharides: Functionality and Prospects. *Int J Mol Sci* 2012; 13(11):14002–15.
- [6] Jindal N, Singh Khattar J. Microbial Polysaccharides in Food Industry. In: Biopolymers for Food Design Elsevier Inc. 2018; pp. 95–123.
- [7] Cruz M, Freitas F, Torres CA V, et al. Influence of temperature on the rheological behavior of a new fucose-containing bacterial exopolysaccharide. *Int J Biol Macromol Elsevier B.V.* 2011; 48(4):695–99.
- [8] Telles CBS, Sabry DA, Almeida-Lima J, et al. Sulfation of the extracellular polysaccharide produced by the edible mushroom *Pleurotus sajor-caju* alters its antioxidant, anticoagulant and antiproliferative properties in vitro. *Carbohydr Polym Elsevier Ltd.* 2011; 85(3):514–21.
- [9] Wang J, Zhao B, Wang X, et al. Synthesis of selenium-containing polysaccharides and evaluation of antioxidant activity in vitro. *Int J Biol Macromol Elsevier B.V.* 2012; 51(5):987–91.
- [10] Suflet DM, Chitanu GC, Desbrires J. Phosphorylated polysaccharides. 2. Synthesis and properties of phosphorylated dextran. *Carbohydr Polym Elsevier Ltd.* 2010; 82(4):1271–77.
- [11] Roca C, Chagas B, Farinha I, et al. Production of yeast chitin-glucan complex from biodiesel industry byproduct. *Process Biochem Elsevier Ltd* 2012; 47(11):1670–75.
- [12] Kollár R, Reinhold BB, Petra E, et al. Architecture of the Yeast Cell Wall. *J Biol Chem* 1997; 272(28):17762–75.
- [13] Kanbe T, Han Y, Redgrave B, et al. Evidence that mannans of *Candida albicans* are responsible for adherence of yeast forms to spleen and lymph node tissue. *Infect Immun* 1993; 61(6):2578–84.
- [14] Parish CR, Freeman C, Brown KJ, et al. Identification of sulfated oligosaccharide-based inhibitors of tumor growth and metastasis using novel in vitro assays for angiogenesis and heparanase activity. *Cancer Res* 1999; 59(14):3433–41.
- [15] Yu G, Gunay NS, Linhardt RJ, et al. Preparation and anticoagulant activity of the phosphosulfomannan PI-88. *Eur J Med Chem* 2002; 37(10):783–91.
- [16] Fukushima K, Tabuani D, Camino G. Nanocomposites of PLA and PCL based on montmorillonite and sepiolite. *Mater Sci Eng C Elsevier B.V.* 2009; 29(4):1433–41.
- [17] Shimao M. Biodegradation of plastics. *Curr Opin Biotechnol* 2001; 12(3):242–47.
- [18] Bunczek, Michael T.; Greenberg, Michael J.; Urnezis, Philip W. Gum Base and Chewing Gum Containing Edible Polyesters. U.S. Patent 6,013,287; (2000).
- [19] Griffith, Nina Cecilia; Ning, Xin; Day, Bryon P.; Aroch, Maya. Compositions For Enhanced Thermal Bonding. U.S. Patent USOO6946195B2; (2005).
- [20] Prasad VS, Pillai CKS. Synthesis, characterization, and in vitro degradation of liquid-crystalline terpolyesters of 4-hydroxyphenylacetic acid/3-(4-hydroxyphenyl)propionic acid with terephthalic acid and 2,6-naphthalene diol. *J Polym Sci Part A Polym Chem* 2002; 40(11):1845–57.
- [21] Mainardes RM, Gremiao MPD, Evangelista RC. Thermoanalytical study of praziquantel-loaded PLGA nanoparticles. *Rev Bras Ciencias Farm* 2006; 42(4):523–30.
- [22] Parrish B, Breitenkamp RB, Emrick T. PEG- and Peptide-Grafted Aliphatic Polyesters by Click Chemistry. *Biomaterials* 2005; 127(17):7404–10.
- [23] Kunasundari B, Sudesh K. Isolation and recovery of microbial polyhydroxyalkanoates. *Express Polym Lett* 2011; 5(7):620–34.
- [24] Madkour MH, Heinrich D, Alghamdi MA, et al. PHA recovery from biomass. *Biomacromolecules* 2013; 14(9):2963–72.
- [25] Heinrich D, Madkour MH, Al-Ghamdi MA, et al. Large scale extraction of poly(3-hydroxybutyrate) from *Ralstonia eutropha* H16 using sodium hypochlorite. *AMB Express* 2012; 2(1):1–6.
- [26] Shang L, Fei Q, Zhang YH, et al. Thermal Properties and Biodegradability Studies of Poly(3-

- hydroxybutyrate-co-3-hydroxyvalerate). *J Polym Environ* 2012; 20(1):23–28.
- [27] Lemos PC, Serafim LS, Reis MAM. Synthesis of polyhydroxyalkanoates from different short-chain fatty acids by mixed cultures submitted to aerobic dynamic feeding. *J Biotechnol* 2006; 122(2):226–38.
- [28] Salehzadeh H, Loosdrecht MCM Van. Production of polyhydroxyalkanoates by mixed culture: Recent trends and biotechnological importance. *Biotechnol Adv* 2004; 22(3):261–79.
- [29] Anseth KS, Bowman CN, Brannon-Peppas L. Mechanical properties of hydrogels and their experimental determination. *Biomaterials* 1996; 17(17):1647–57.
- [30] Hoffman AS. Hydrogels for biomedical applications. *Adv Drug Deliv Rev Elsevier B.V.* 2012; 64(SUPPL.):18–23.
- [31] Nazir A, Asghar A, Aslam Maan A. Chapter 13 - Food Gels: Gelling Process and New Applications. In: *Advances in Food Rheology and Its Applications Elsevier Ltd* 2017; pp. 335–353.
- [32] Auffan M, Rose J, Wiesner MR, et al. Chemical stability of metallic nanoparticles: A parameter controlling their potential cellular toxicity in vitro. *Environ Pollut* 2009; 157(4):1127–33.
- [33] Freitas F, Alves VD, Reis MAM. Advances in bacterial exopolysaccharides: From production to biotechnological applications. *Trends Biotechnol Elsevier Ltd* 2011; 29(8):388–98.
- [34] Alves VD, Torres CAV, Freitas F. Bacterial polymers as materials for the development of micro/nanoparticles. *Int J Polym Mater Polym Biomater* 2016; 65(5):211–24.
- [35] Alizadeh A, Behfar S. Properties of collagen based edible films in food packaging: A review. *Sch Res Libr Ann Biol Res* 2013; 4(2):253–56.
- [36] Bassi P, Kaur G. Polymeric films as a promising carrier for bioadhesive drug delivery: Development, characterization and optimization. *Saudi Pharm J King Saud University* 2017; 25(1):32–43.
- [37] Cai Q, Yang J, Bei J, et al. A novel porous cells scaffold made of polylactide-dextran blend by combining phase-separation and particle-leaching techniques. *Biomaterials* 2002; 23(23):4483–92.
- [38] Garg T, Singh O, Arora S, et al. Scaffold: A Novel Carrier for Cell and Drug Delivery. *Crit Rev Ther Drug Carr Syst* 2012; 29(1):1–63.
- [39] Shishatskaya EI, Volova TG. A comparative investigation of biodegradable polyhydroxyalkanoate films as matrices for in vitro cell cultures. *J Mater Sci Mater Med* 2004; 15(8):915–23.
- [40] Zhijiang C, Guang Y, Kim J. Biocompatible nanocomposites prepared by impregnating bacterial cellulose nanofibrils into poly(3-hydroxybutyrate). *Curr Appl Phys Elsevier B.V* 2011; 11(2):247–49.
- [41] Zhijiang C, Chengwei H, Guang Y. Poly(3-hydroxybutyrate-co-4-hydroxybutyrate)/bacterial cellulose composite porous scaffold: Preparation, characterization and biocompatibility evaluation. *Carbohydr Polym Elsevier Ltd.* 2012; 87(2):1073–80.
- [42] Freitas MFA de, Roca CFA, Cruz FM da S, et al. Natural Biocomposite Powder Prepared from *Pichia pastoris* Biomass, Method of Preparation and Its Use as Excipient. U.S. Patent 20130251806A1; (2013).
- [43] Jones D.B, Factors for converting percentages of nitrogen in foods and feeds into percentages of protein. US Department of Agriculture-circ. 183. Washington, DC. 1941.
- [44] DiLuzio NR. Soluble Phosphorylated Glucan. U.S. Patent 4,877,777 (1989).
- [45] Zhang M, Su N, Huang Q, et al. Phosphorylation and antiaging activity of polysaccharide from *Trichosanthes* peel. *J Food Drug Anal Elsevier Ltd* 2017; 25(4):976–83.
- [46] Okubo Y, Ichikawa T, Suzuki S. Relationship between phosphate content and immunochemical properties of subfractions of bakers' yeast mannan. *J Bacteriol* 1978; 136(1):63–68.
- [47] Okubo Y, Honma Y, Suzuki S. Relationship between phosphate content and serological activities of the mannans of *Candida albicans* strains NIH A-207, NIH B-792 and J-1012. *J Bacteriol* 1979; 137(1):677–80.
- [48] Masuoka J, Hazen KC. Cell wall mannan and cell surface hydrophobicity in *Candida albicans* serotype A and B strains. *Infect Immun* 2004; 72(11):6230–36.
- [49] Ferro V, Li C, Fewings K, et al. Determination of the composition of the oligosaccharide phosphate fraction of *Pichia (Hansenula) holstii* NRRL Y-2448 phosphomannan by capillary electrophoresis and HPLC. *Carbohydr Res* 2002; 337(2):139–46.
- [50] Huang GL, Yang Q, Wang ZB. Extraction and deproteinization of mannan oligosaccharides. *Zeitschrift fur Naturforsch - Sect C J Biosci* 2010; 65 C(5–6):387–90.
- [51] Deng C, Fu H, Xu J, et al. Physicochemical and biological properties of phosphorylated polysaccharides from *Dictyophora indusiata*. *Int J Biol Macromol Elsevier B.V.* 2015; 72:894–

- 99.
- [52] Treenate P. The Effect of Glycerol/Water and Sorbitol/Water on the Plasticization of Hydroxyethylacryl Chitosan/Sodium Alginate Films. MATEC Web Conf 2015; 6:P1–4.
 - [53] Gamba AM, Fonseca JS, Méndez DA, et al. Assessment of different plasticizer - Polyhydroxyalkanoate mixtures to obtain biodegradable polymeric films. Chem Eng Trans 2017; 57:1363–68.
 - [54] Chen LJ, Wang M. Production and evaluation of biodegradable composites based on PHB-PHV copolymer. Biomaterials 2002; 23(13):2631–39.
 - [55] Martin P. Wound Healing--Aiming for Perfect Skin Regeneration. Science (80-) 1997; 276(5309):75–81.
 - [56] Alves A, Sousa RA, Reis RL. In vitro cytotoxicity assessment of ulvan, a polysaccharide extracted from green algae. Phyther Res 2013; 27(8):1143–48.